Gravitational waves from the first order electroweak phase transition in the Z_3 symmetric singlet scalar model

Toshinori Matsui[1]

in collaborated with Zhaofeng Kang[2] and Pyungwon Ko[1]

[1]Korea Institute for Advanced Study (KIAS)

[2]Huazhong University of Science and Technology

Z. Kang, P. Ko and TM, arXiv:1706.09721 [hep-ph]

Motivation

- Discovery of the Higgs boson
  - Mass generation mechanism is confirmed
  - The standard model as an effective theory is established
- What is the nature of electroweak symmetry breaking?
  - SM have minimal Higgs potential…**no principle**
  - Higgs self-couplings **have not been measured**

    →We have not understood the shape of the Higgs potential

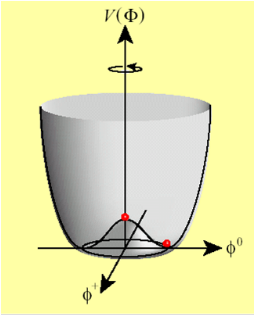

- Exploring the structure of the Higgs sector is important
  - New physics is required to solve BSM phenomena

    Baryon asymmetry of the Universe, Existence of dark matter,…
  - BSM might be related to the extended Higgs sector

    EW baryogenesis, Radiative neutrino mass models, …

Electroweak Baryogenesisa

~ Importance to understand the Higgs potential ~

- Observed Baryon number: $\boxed{n_B/s \simeq \mathcal{O}(10^{-10})}$
- Sakharov's three conditions

1. #B violation, 2. CP violation, 3. Departure from equilibrium

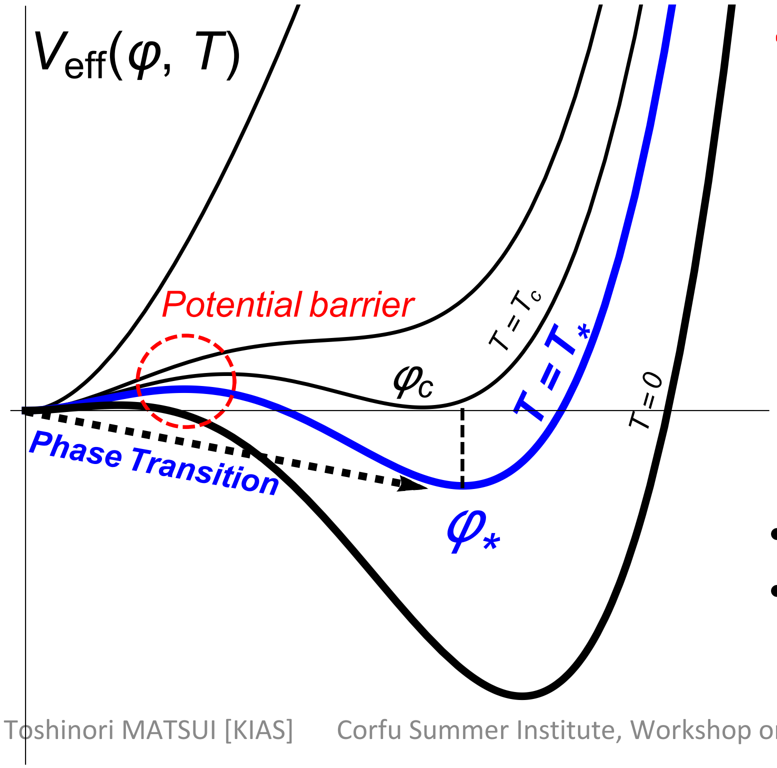

→Strongly 1st order phase transition

$$\boxed{\varphi_*/T_* \gtrsim 1}$$

- SM (m_h=125GeV) cannot satisfy these conditions.
- Strongly 1stOPT is realized by models with extended Higgs sector.

Strongly 1st order Phase transition

The strength of phase transition

$$\boxed{\frac{\varphi_c}{T_c} = \frac{2E}{\lambda}(1 - \frac{e\lambda}{ET})}$$

(analytic formula of couplings are given by one field & high-T approx.)

$$V_{\rm eff} = D(T^2 - T_0^2)\varphi^2 - (\underline{ET - e})\varphi^3 + \frac{\lambda(T)}{4}\varphi^4$$

Strongly 1st order Phase transition

The strength of phase transition

$$\boxed{\frac{\varphi_c}{T_c} = \frac{2E}{\lambda}\left(1 - \frac{e\lambda}{ET}\right)}$$

(analytic formula of couplings are given by one field & high-T approx.)

$$V_{\rm eff} = D(T^2 - T_0^2)\varphi^2 - (\underline{ET - e})\varphi^3 + \frac{\lambda(T)}{4}\varphi^4$$

e.g. Inert Singlet Model

Inert Singlet Model (real singlet scalar with Z_2 sym.)

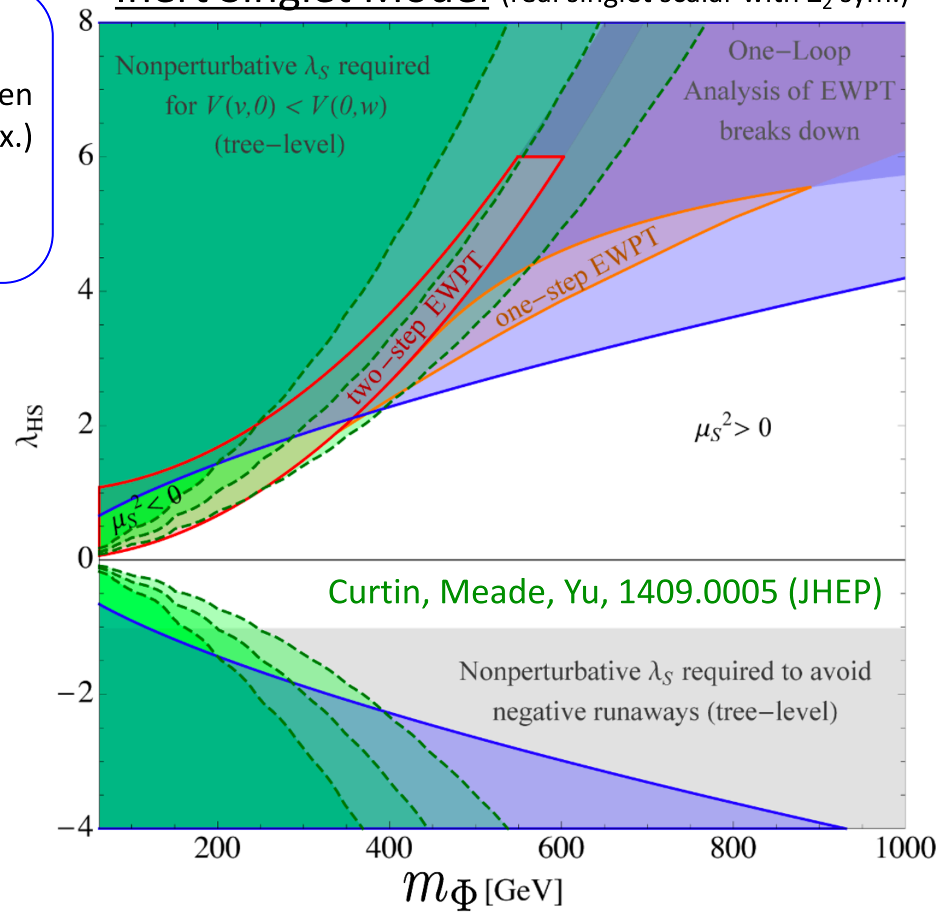

Strongly 1st order Phase transition

The strength of phase transition

$$\boxed{\frac{\varphi_c}{T_c} = \frac{2E}{\lambda}\left(1 - \frac{e\lambda}{ET}\right)}$$

(analytic formula of couplings are given by one field & high-T approx.)

$$V_{\rm eff} = D(T^2 - T_0^2)\varphi^2 - (ET - e)\varphi^3 + \frac{\lambda(T)}{4}\varphi^4$$

e.g. Inert Singlet Model (one-step EWPT)

$$\boxed{E = \frac{1}{12\pi v^3}\left\{6m_{W^\pm}^3 + 3m_Z^3 + \sum_{\Phi} m_\Phi^3 \left(1 - \frac{M^2}{m_\Phi^2}\right)^3 \left(1 + \frac{3}{2}\frac{M^2}{m_\Phi^2}\right)\right\}}$$

$$m_\Phi^2 \simeq M^2 + \lambda_{HS} v^2$$

Both are enhanced by $M \to 0$ limit (large λ_{HS})

Inert Singlet Model (real singlet scalar with Z_2 sym.)

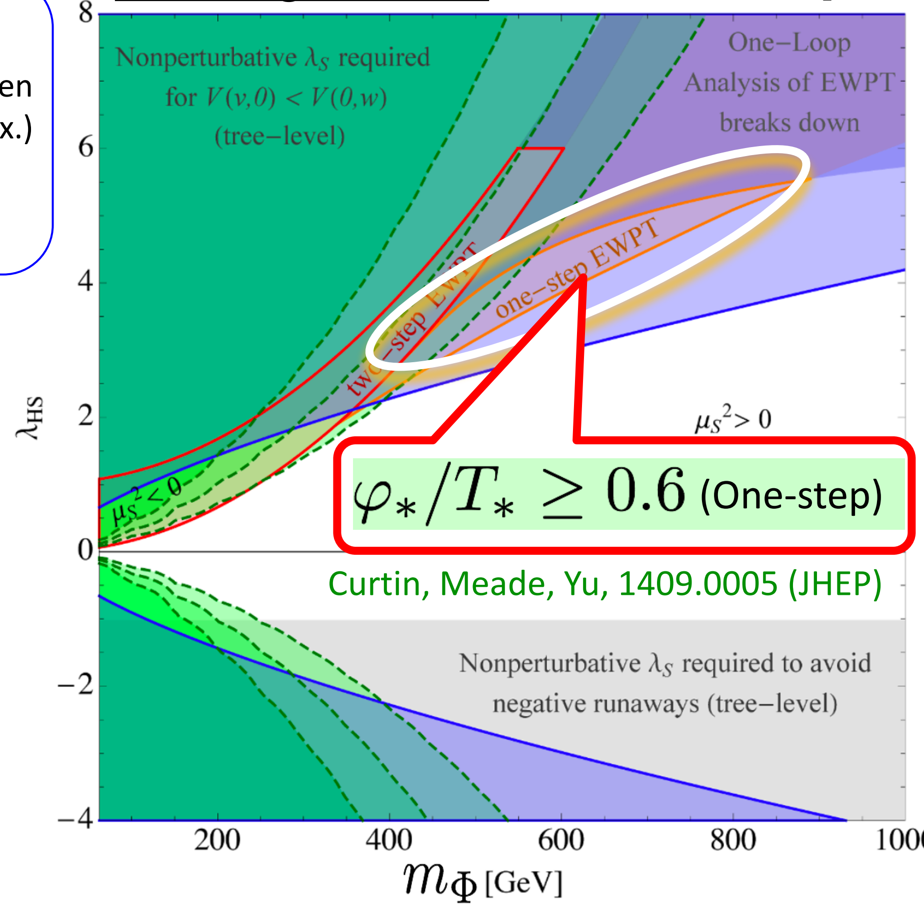

Strongly 1st order Phase transition

The strength of phase transition

$$\boxed{\frac{\varphi_c}{T_c} = \frac{2E}{\lambda}\left(1 - \frac{e\lambda}{ET}\right)}$$

(analytic formula of couplings are given by one field & high-T approx.)

$$V_{\text{eff}} = D(T^2 - T_0^2)\varphi^2 - (\underline{ET - e})\varphi^3 + \frac{\lambda(T)}{4}\varphi^4$$

e.g. Inert Singlet Model (one-step EWPT)

$$\boxed{E = \frac{1}{12\pi v^3}\left\{6m_{W^\pm}^3 + 3m_Z^3 + \sum_\Phi m_\Phi^3 \left(1 - \frac{M^2}{m_\Phi^2}\right)^3 \left(1 + \frac{3}{2}\frac{M^2}{m_\Phi^2}\right)\right\}}$$

$$\boxed{\frac{\Delta\lambda_{hhh}}{\lambda_{hhh}} \equiv \frac{\lambda_{hhh} - \lambda_{hhh}^{\text{SM}}}{\lambda_{hhh}^{\text{SM}}}}$$

$$\boxed{\lambda_{hhh}^{\text{2HDM}} \equiv \frac{3m_h^2}{v}\left\{1 - \frac{m_t^4}{\pi^2 m_h^2 v^2} + \sum_\Phi \frac{m_\Phi^4}{12\pi^2 m_h^2 v^2}\left(1 - \frac{M^2}{m_\Phi^2}\right)\right\}}$$

$$m_\Phi^2 \simeq M^2 + \lambda_{HS} v^2$$

Both are enhanced by $M \to 0$ limit (large λ_{HS})

Inert Singlet Model (real singlet scalar with Z_2 sym.)

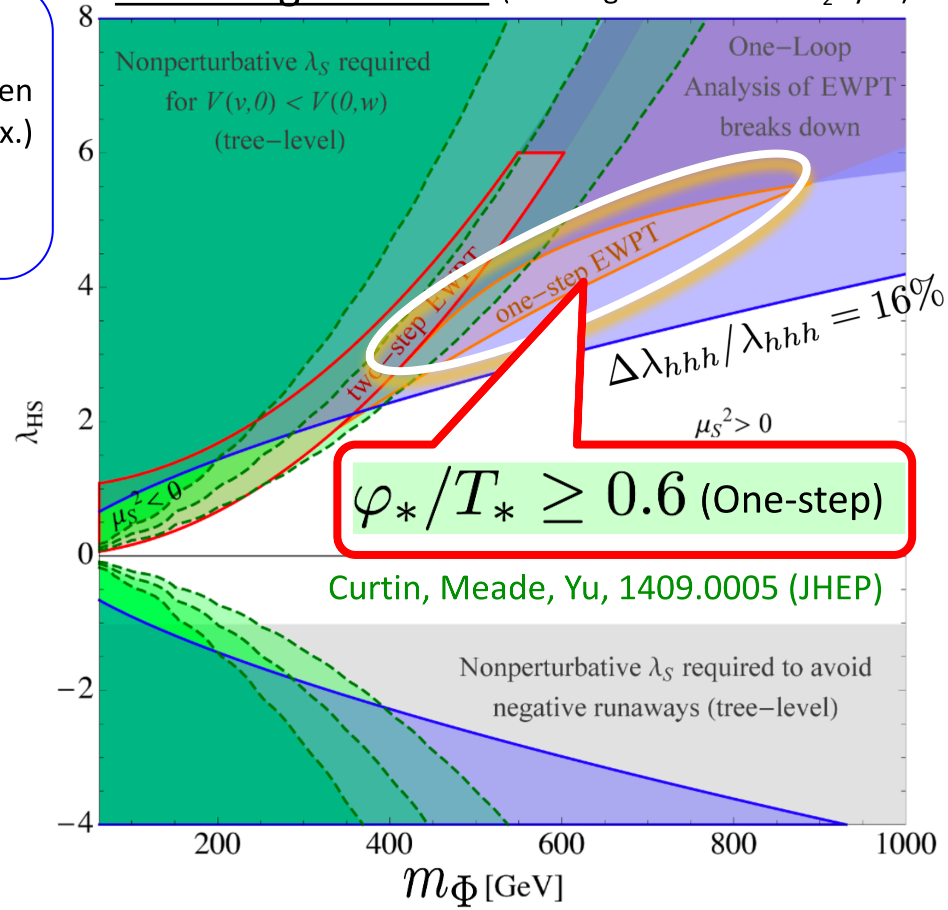

Large deviation in the *hhh* coupling is required! → EWPT can be tested at future colliders!

Strongly 1st order Phase transition

The strength of phase transition

$$\frac{\varphi_c}{T_c} = \frac{2E}{\lambda}\left(1 - \frac{e\lambda}{ET}\right)$$

(analytic formula of couplings are given by one field & high-T approx.)

$$V_{\text{eff}} = D(T^2 - T_0^2)\varphi^2 - (ET - e)\varphi^3 + \frac{\lambda(T)}{4}\varphi^4$$

e.g. Inert Singlet Model (one-step EWPT)

$$E = \frac{1}{12\pi v^3}\left\{6m_{W^\pm}^3 + 3m_Z^3 + \sum_\Phi m_\Phi^3 \left(1 - \frac{M^2}{m_\Phi^2}\right)^3 \left(1 + \frac{3}{2}\frac{M^2}{m_\Phi^2}\right)\right\}$$

$$\frac{\Delta\lambda_{hhh}}{\lambda_{hhh}} \equiv \frac{\lambda_{hhh} - \lambda_{hhh}^{\text{SM}}}{\lambda_{hhh}^{\text{SM}}}$$

$$\lambda_{hhh}^{\text{2HDM}} \equiv \frac{3m_h^2}{v}\left\{1 - \frac{m_t^4}{\pi^2 m_h^2 v^2} + \sum_\Phi \frac{m_\Phi^4}{12\pi^2 m_h^2 v^2}\left(1 - \frac{M^2}{m_\Phi^2}\right)\right\}$$

$$m_\Phi^2 \simeq M^2 + \lambda_{HS} v^2$$

Both are enhanced by $M \to 0$ limit (large λ_{HS})

Inert Singlet Model (real singlet scalar with Z_2 sym.)

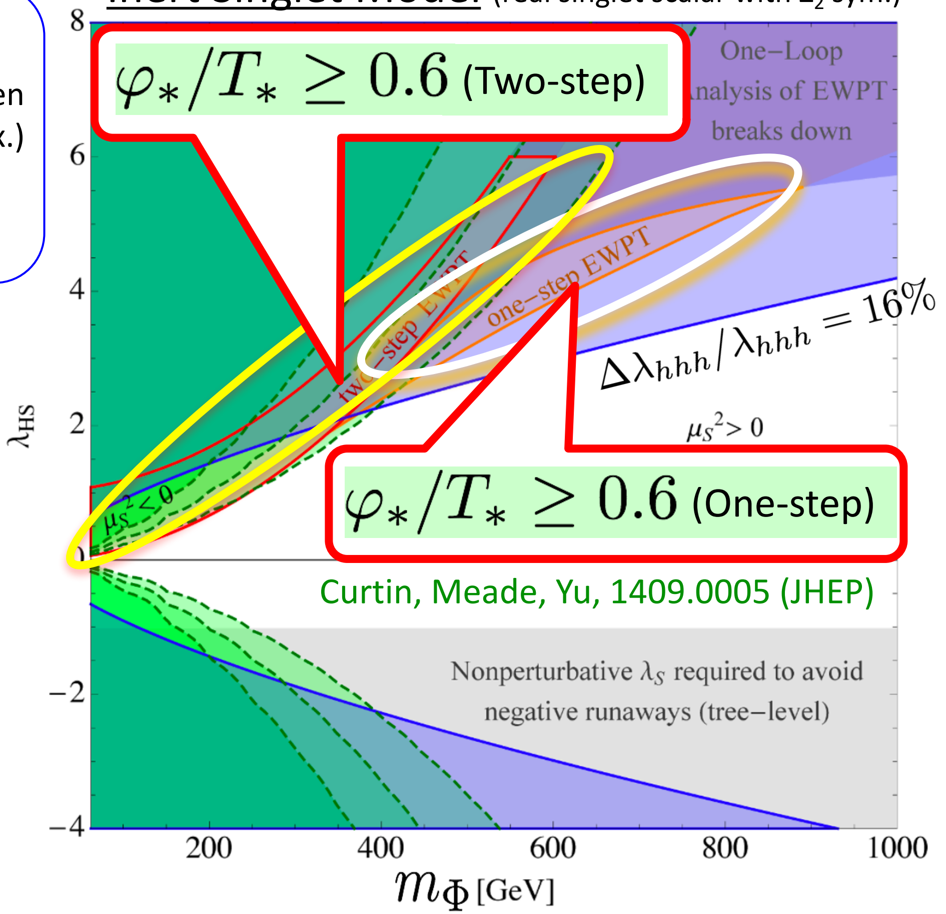

Large deviation in the *hhh* coupling is required! → EWPT can be tested at future colliders!

Strongly 1st order Phase transition

The strength of phase transition

$$\boxed{\frac{\varphi_c}{T_c} = \frac{2E}{\lambda}\left(1 - \frac{e\lambda}{ET}\right)}$$

(analytic formula of couplings are given by one field & high-T approx.)

$$V_{\rm eff} = D(T^2 - T_0^2)\varphi^2 - (\underline{ET - e})\varphi^3 + \frac{\lambda(T)}{4}\varphi^4$$

e.g. Inert Singlet Model (one-step EWPT)

$$E = \frac{1}{12\pi v^3}\left\{6m_{W^\pm}^3 + 3m_Z^3 + \sum_\Phi m_\Phi^3\left(1 - \frac{M^2}{m_\Phi^2}\right)^3\left(1 + \frac{3}{2}\frac{M^2}{m_\Phi^2}\right)\right\}$$

$$\frac{\Delta\lambda_{hhh}}{\lambda_{hhh}} \equiv \frac{\lambda_{hhh} - \lambda_{hhh}^{\rm SM}}{\lambda_{hhh}^{\rm SM}}$$

$$\lambda_{hhh}^{\rm 2HDM} \equiv \frac{3m_h^2}{v}\left\{1 - \frac{m_t^4}{\pi^2 m_h^2 v^2} + \sum_\Phi \frac{m_\Phi^4}{12\pi^2 m_h^2 v^2}\left(1 - \frac{M^2}{m_\Phi^2}\right)^3\right\}$$

$$m_\Phi^2 \simeq M^2 + \lambda_{HS} v^2$$

Both are enhanced by $M \to 0$ limit (large λ_{HS})

Inert Singlet Model (real singlet scalar with Z_2 sym.)

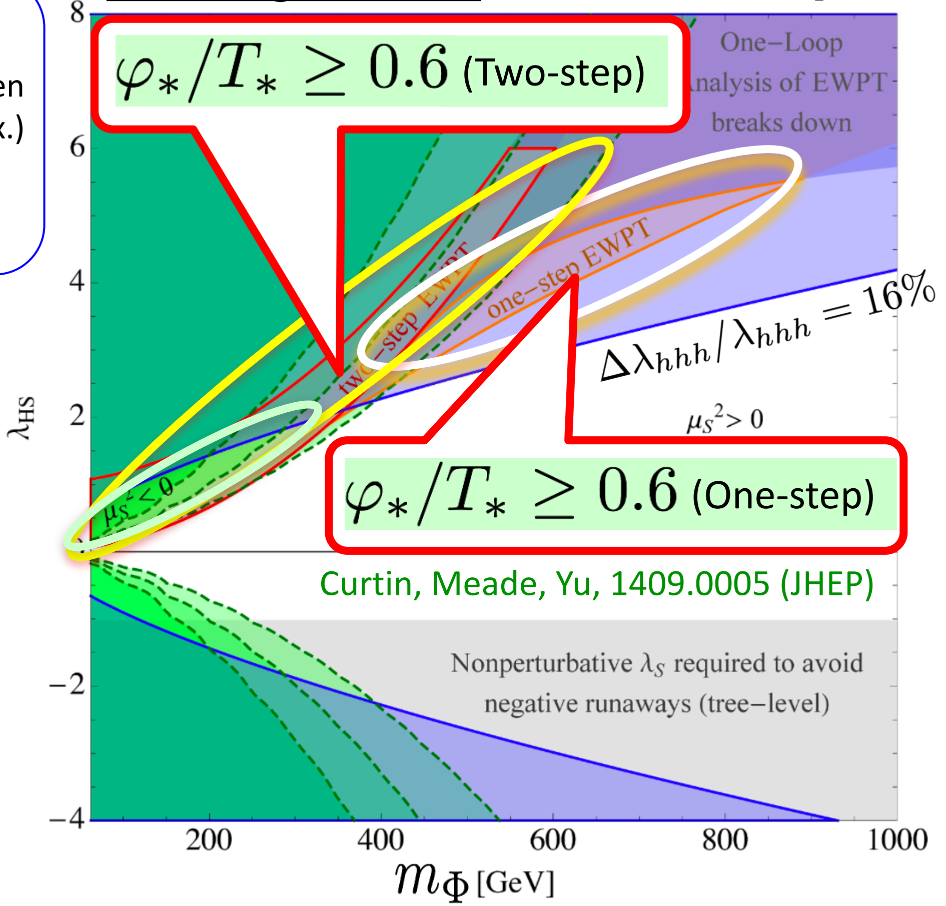

Large deviation in the *hhh* coupling is required! → EWPT can be tested at future colliders!

Nightmare scenario

- Potential barrier with 1stOPT can be created even if the Higgs couplings do not deviate from SM.

- In the model with the unbroken discrete symmetry (such as Z_2, Z_3, …), the strongly 1stOPT can be realized by multi-step PT. In such a case, it is difficult to test at colliders in a part of parameter regions.

- We expect the observations of the gravitational waves as a new technique to detect the signal of the strongly 1stOPT.

Gravitational waves

～ Probing the Higgs potential by GW observations ～

Sensitivity of GW detectors

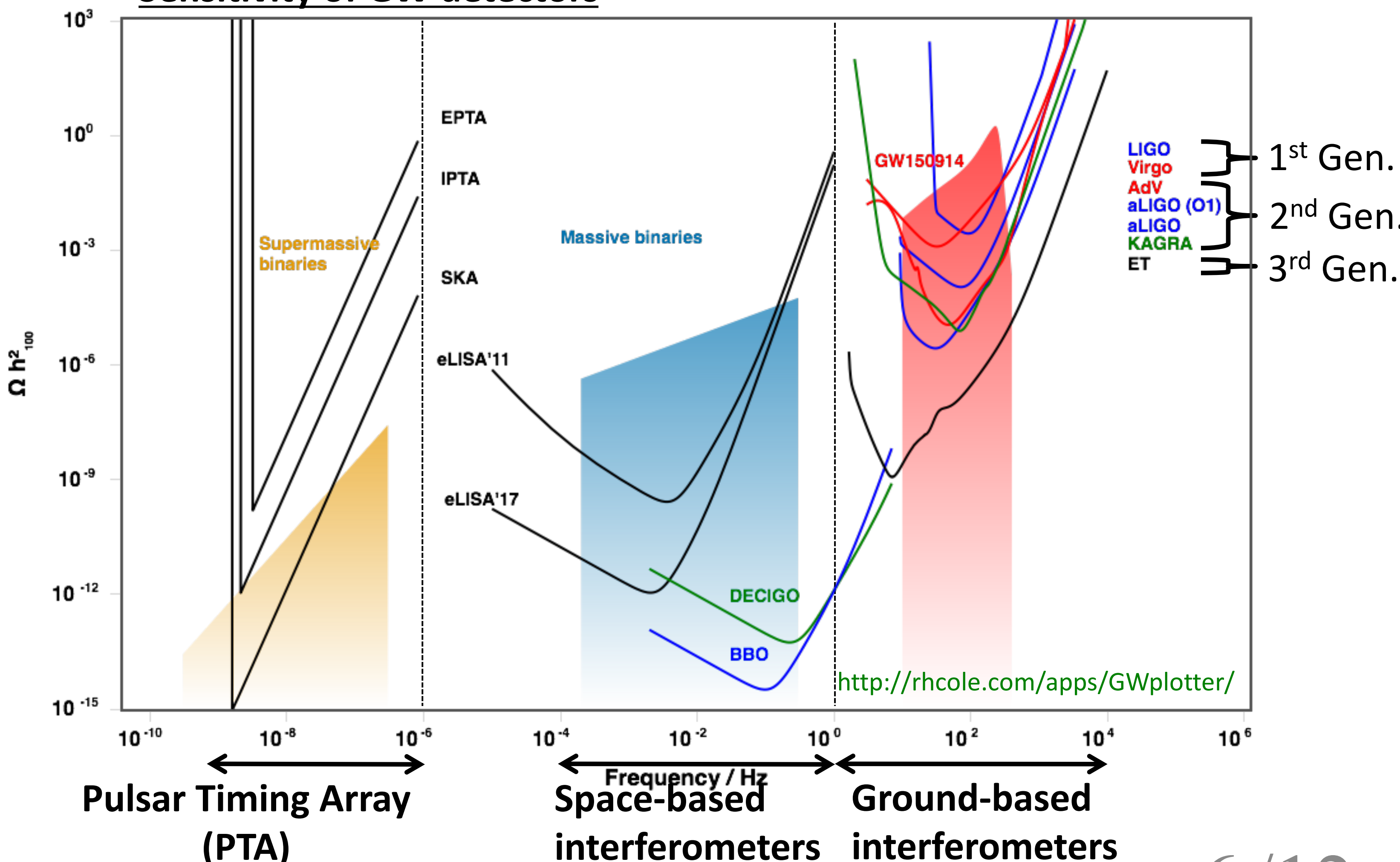

Gravitational waves

～ Probing the Higgs potential by GW observations ～

Sensitivity of GW detectors

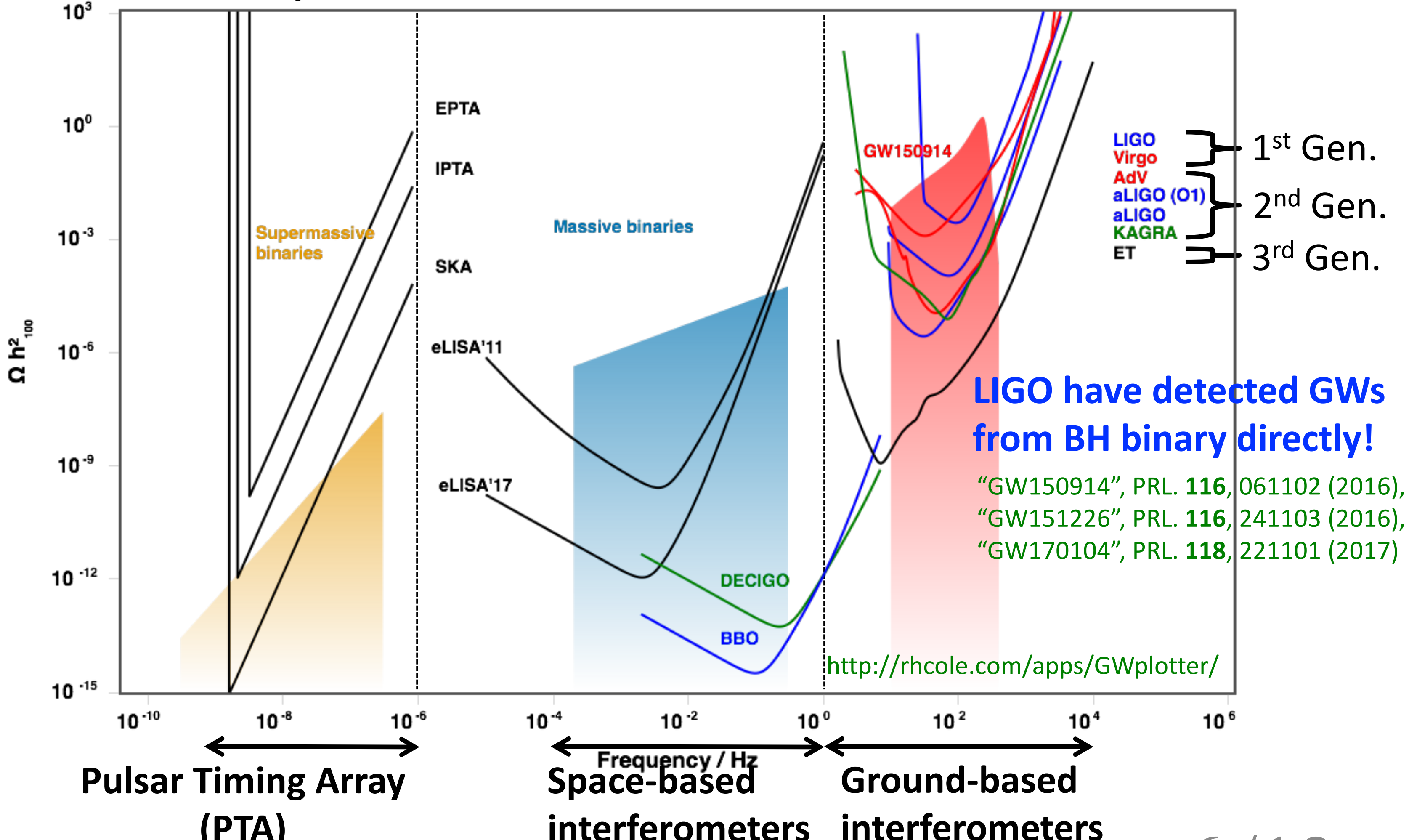

Gravitational waves

～ Probing the Higgs potential by GW observations ～

Sensitivity of GW detectors

Red shifted frequency:

$$\boxed{f_0 = \frac{a_t}{a_0} f_t}$$

EWPT (~100GeV)

$$f_0 \simeq 10^{-5}\mathrm{Hz}\frac{T_t}{100\mathrm{GeV}}\frac{f_t}{H_t}$$

$$\frac{f_t}{H_t} \simeq \frac{H_t^{-1}}{\lambda_t} = 100 - 1000$$

EWPT can be explored at future space-based interferometers!

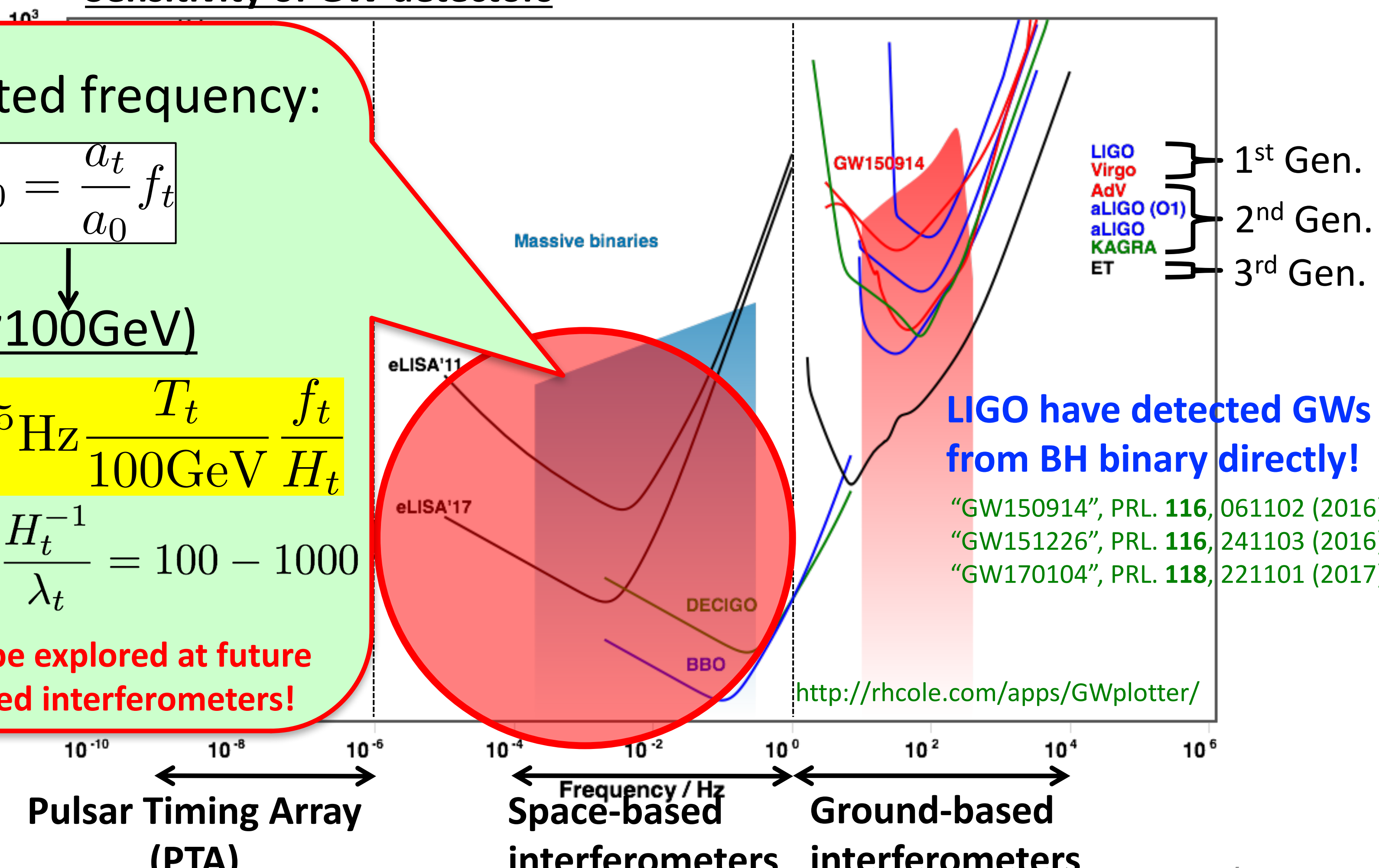

LIGO have detected GWs from BH binary directly!

"GW150914", PRL. **116**, 061102 (2016),
"GW151226", PRL. **116**, 241103 (2016),
"GW170104", PRL. **118**, 221101 (2017)

GWs from 1stOPT

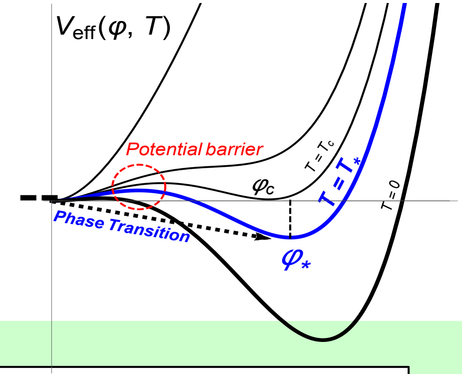

$V_{\text{eff}}(\varphi, T)$ (Model)

GWs from 1stOPT

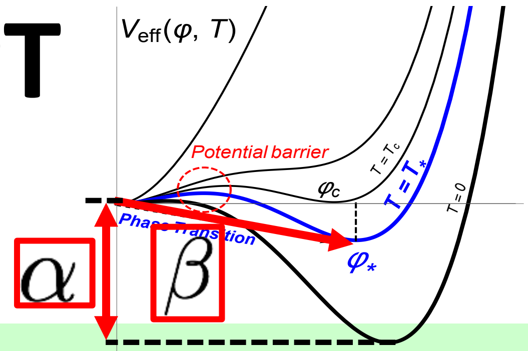

$V_{\rm eff}(\varphi, T)$ (Model)

↓

$\alpha, \tilde{\beta}$ @T=T_t

<u>Characteristic parameters of 1stOPT</u>

- α is defined as $\alpha \equiv \left.\frac{\epsilon}{\rho_{\rm rad}}\right|_{T=T_t}$. ($\rho_{\rm rad}$ is energy density of rad.)
  - Latent heat: $\epsilon(T) \equiv -\Delta V_{\rm eff}(\varphi_B(T), T) + T\frac{\partial \Delta V_{\rm eff}(\varphi_B(T))}{\partial T}$

  α ~ "Normalized difference of the potential minima"

- β is defined as $\beta \equiv \left.\frac{1}{\Gamma}\frac{d\Gamma}{dt}\right|_{t=t_t}$. → $\tilde{\beta}\left(\equiv \frac{\beta}{H_t}\right) = T_t \left.\frac{d(S_3(T)/T)}{dT}\right|_{T=T_t}$
  - Bubble nucleation rate: $\Gamma(T) \simeq T^4 e^{-\frac{S_3(T)}{T}}$
  - 3-dim. Euclidean action: $S_3(T) = \int dr^3 \left\{\frac{1}{2}\left(\vec{\nabla}\varphi\right)^2 + V_{\rm eff}(\varphi, T)\right\}$

  β^{-1} ~ "Transition time"

GWs from 1^{st}OPT

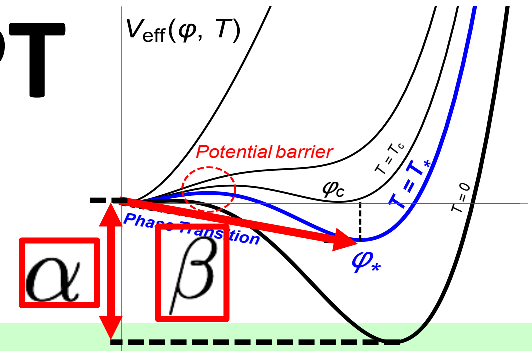

Characteristic parameters of 1^{st}OPT

- α is defined as $\alpha \equiv \left.\frac{\epsilon}{\rho_{\rm rad}}\right|_{T=T_t}$. ($\rho_{\rm rad}$ is energy density of rad.)
  - Latent heat: $\epsilon(T) \equiv -\Delta V_{\rm eff}(\varphi_B(T),T) + T\frac{\partial \Delta V_{\rm eff}(\varphi_B(T))}{\partial T}$

  α ~ "Normalized difference of the potential minima"

- β is defined as $\beta \equiv \left.\frac{1}{\Gamma}\frac{d\Gamma}{dt}\right|_{t=t_t}$. $\rightarrow \tilde{\beta}\left(\equiv \frac{\beta}{H_t}\right) = T_t \left.\frac{d(S_3(T)/T)}{dT}\right|_{T=T_t}$
  - Bubble nucleation rate: $\Gamma(T) \simeq T^4 e^{-\frac{S_3(T)}{T}}$
  - 3-dim. Euclidean action: $S_3(T) = \int dr^3 \left\{\frac{1}{2}\left(\vec{\nabla}\varphi\right)^2 + V_{\rm eff}(\varphi,T)\right\}$

  β^{-1} ~ "Transition time"

$V_{\rm eff}(\varphi, T)$ (Model)

↓

$\alpha, \tilde{\beta}$ @T=T_t

↓ Prediction*

$\Omega_{\rm GW}(f)h^2$ (Observable)

(*) C. Caprini *et al.*, JCAP**1604**, 001 (2016)

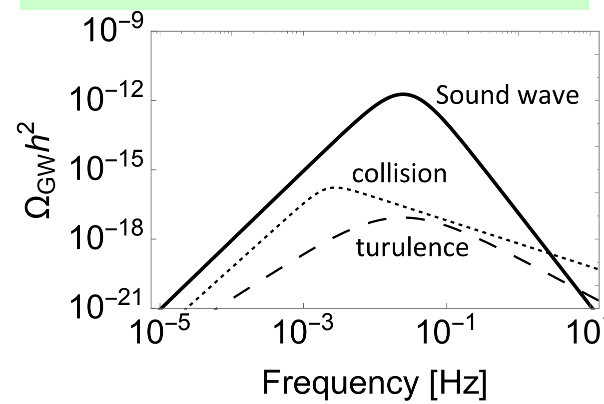

Three sources of GWs (relic abundance @ peak frequency)

"Sound waves" (Compressional plasma)
"Bubble collision" (Envelope approximation)
"Magnetohydrodynamic turbulence in the plasma"

Z_3-symmetric model

- Higgs potential

$$V_0 = -\mu_h^2|H|^2 - \mu_s^2|S|^2 + \lambda_h|H|^4 + \lambda_s|S|^4 + \sqrt{2}\left(\frac{A_s}{3}S^3 + \text{h.c.}\right) + \lambda_{sh}|H|^2|S|^2$$

  – complex singlet scalar: $S \to e^{i2w}S$ with $w = \pi/3$

- Phase transition patterns
  – One-step ($\mu_s^2 > 0$, largeλ_{sh})
    $\Omega_0 \to \Omega_h$
  – Two-step ($\mu_s^2 < 0$)
    $\Omega_0 \to \Omega_s \to \Omega_h$
  – Three-step
    $\Omega_0 \to \Omega_s \to \Omega_{sh} \to \Omega_h$

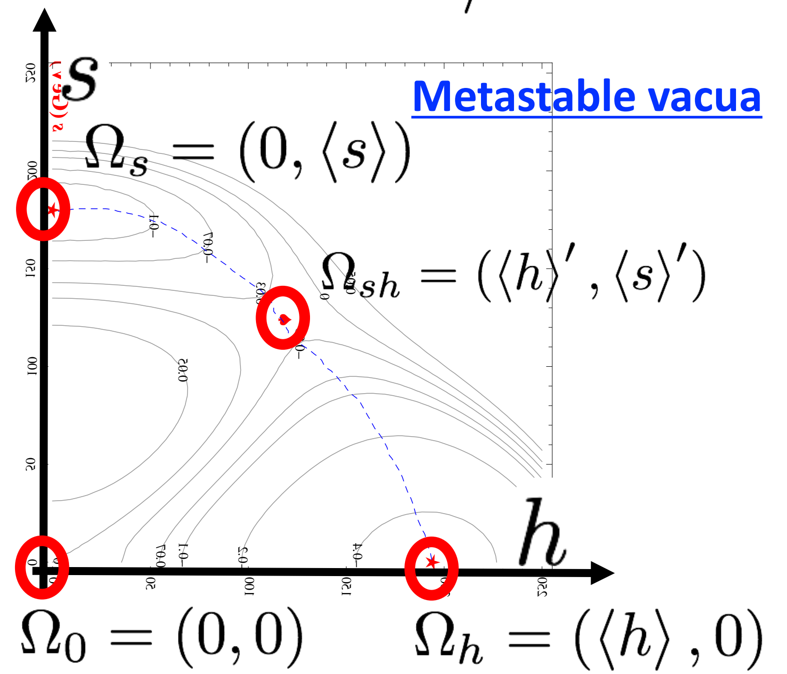

Z_3-symmetric model

- Higgs potential

$$V_0 = -\mu_h^2|H|^2 - \mu_s^2|S|^2 + \lambda_h|H|^4 + \lambda_s|S|^4 + \sqrt{2}\underline{\left(\frac{A_s}{3}S^3 + \text{h.c.}\right)} + \lambda_{sh}|H|^2|S|^2$$

  – complex singlet scalar: $S \to e^{i2w}S$ with $w = \pi/3$

- Phase transition patterns
  – One-step ($\mu_s^2 > 0$, largeλ_{sh})
  $\Omega_0 \to \Omega_h$

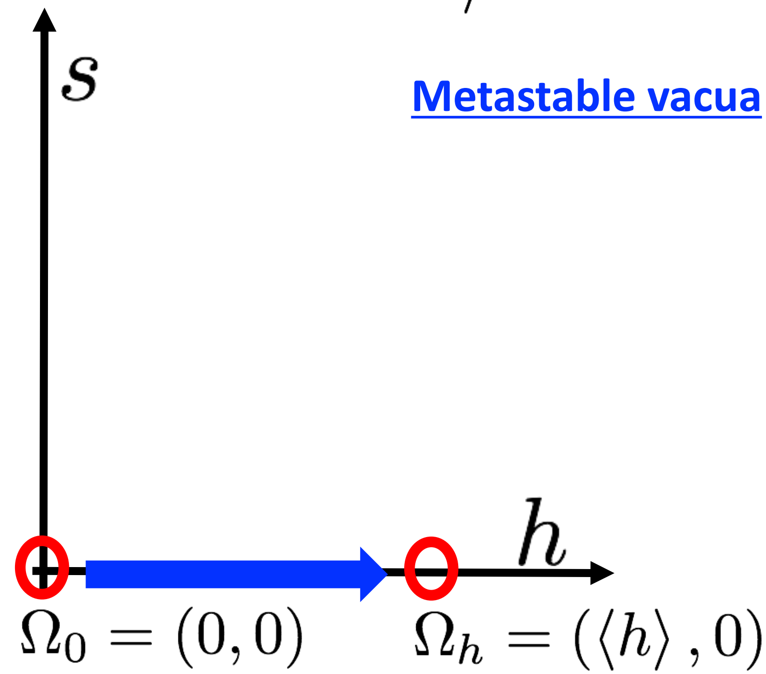

Metastable vacua

Z_3-symmetric model

- Higgs potential

$$V_0 = -\mu_h^2|H|^2 - \mu_s^2|S|^2 + \lambda_h|H|^4 + \lambda_s|S|^4 + \sqrt{2}\underline{\left(\frac{A_s}{3}S^3 + \text{h.c.}\right)} + \lambda_{sh}|H|^2|S|^2$$

  – complex singlet scalar: $S \to e^{i2w}S$ with $w = \pi/3$

- Phase transition patterns

  – Two-step ($\mu_s^2 < 0$)

  $\Omega_0 \to \Omega_s \to \Omega_h$

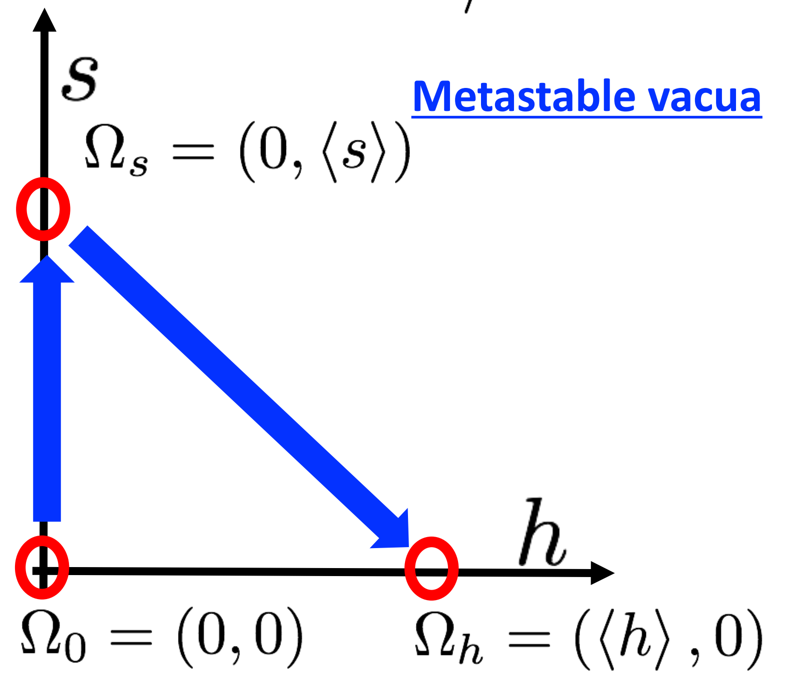

Z_3-symmetric model

- Higgs potential

$$V_0 = -\mu_h^2|H|^2 - \mu_s^2|S|^2 + \lambda_h|H|^4 + \lambda_s|S|^4 + \sqrt{2}\left(\frac{A_s}{3}S^3 + \text{h.c.}\right) + \lambda_{sh}|H|^2|S|^2$$

  – complex singlet scalar: $S \to e^{i2w}S$ with $w = \pi/3$

- Phase transition patterns

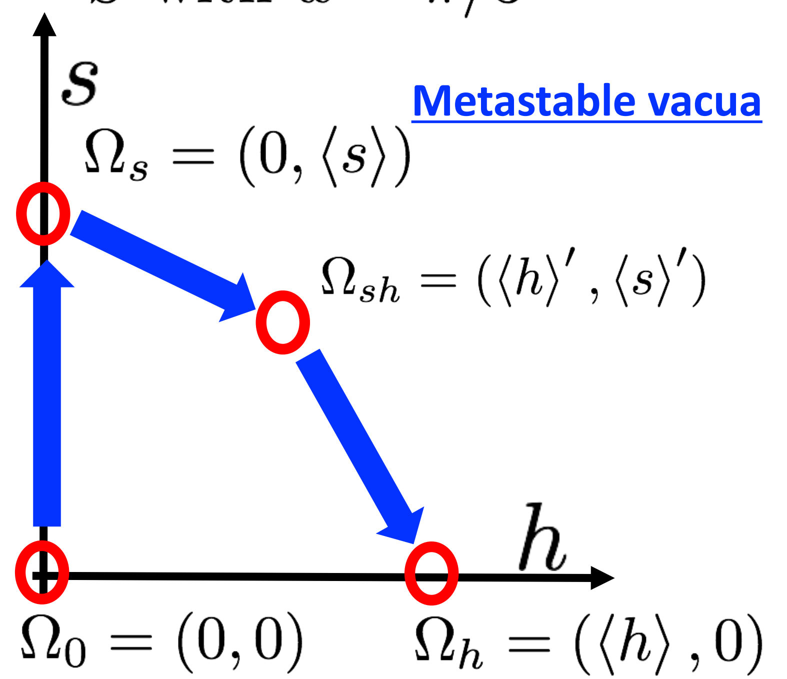

  – Three-step

$$\Omega_0 \to \Omega_s \to \Omega_{sh} \to \Omega_h$$

Z_3-symmetric model

- Higgs potential

$$V_0 = -\mu_h^2|H|^2 - \mu_s^2|S|^2 + \lambda_h|H|^4 + \lambda_s|S|^4 + \sqrt{2}\left(\frac{A_s}{3}S^3 + \text{h.c.}\right) + \lambda_{sh}|H|^2|S|^2$$

  – complex singlet scalar: $S \to e^{i2w}S$ with $w = \pi/3$

- Phase transition patterns
  – One-step ($\mu_s^2 > 0$, largeλ_{sh})
  $\Omega_0 \to \Omega_h$
  – Two-step ($\mu_s^2 < 0$)
  $\Omega_0 \to \Omega_s \to \Omega_h$
  – Three-step
  $\Omega_0 \to \Omega_s \to \Omega_{sh} \to \Omega_h$

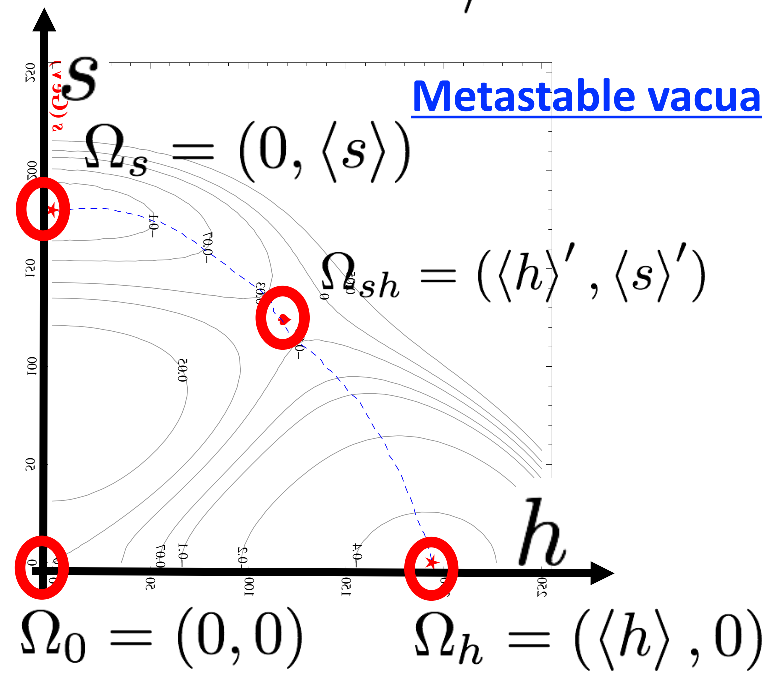

Allowed region of strongly 1st OPT via multi-step PT

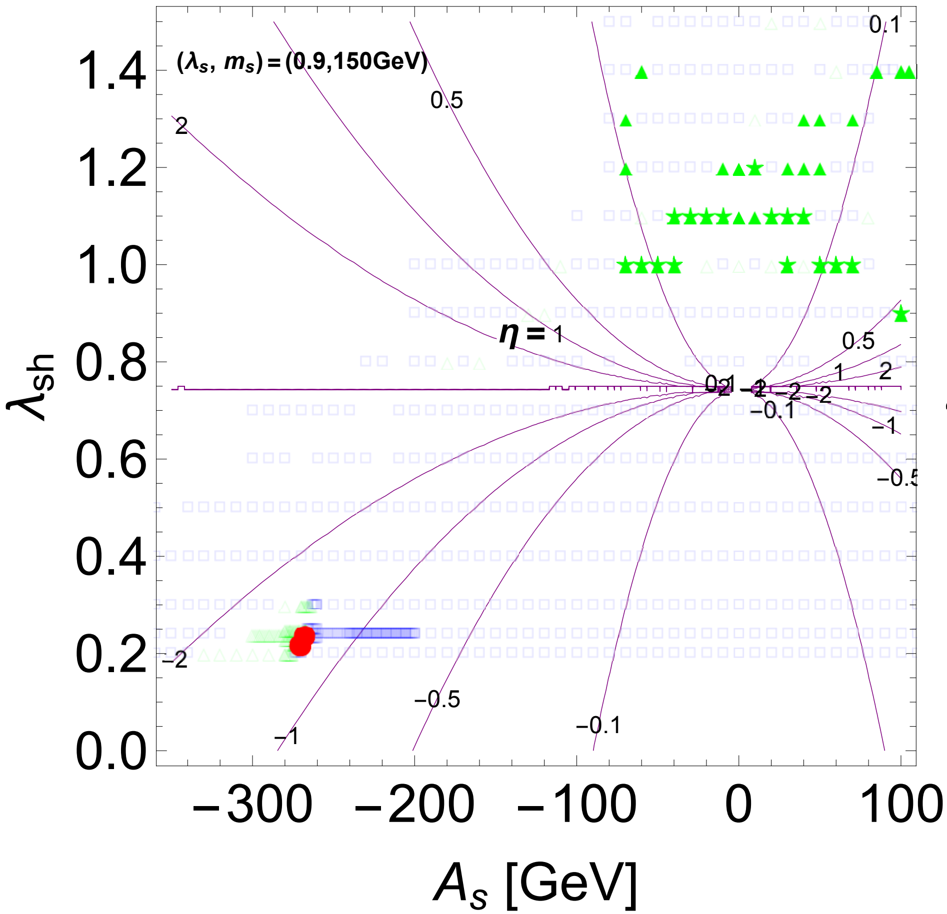

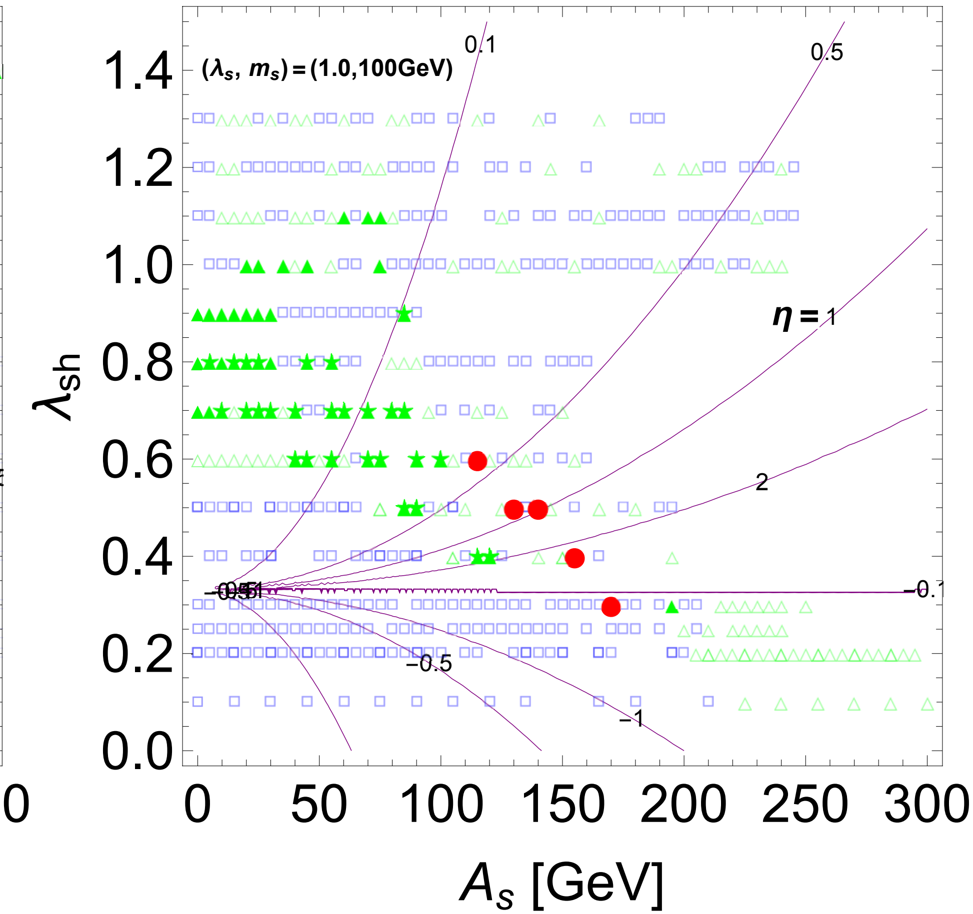

<u>Strongly 1st order phase transitions</u> <u>with multi-step</u>

▲: Two-step PT (Z_2-like case), ★: Two-step PT (large A_s case), ●: Three-step PT

$\Omega_0 \xrightarrow{\text{2nd}} \Omega_s \xrightarrow{\text{1st}} \Omega_h$ $\Omega_0 \xrightarrow{\text{1st}} \Omega_s \xrightarrow{\text{1st}} \Omega_h$ $\Omega_0 \xrightarrow{\text{1st}} \Omega_s \xrightarrow{\text{2nd}} \Omega_{sh} \xrightarrow{\text{1st}} \Omega_h$

□: 2nd order EWPT (one-step)

Transition temperatures

Two step PT (Z_2-like case)

$$\Omega_0 \xrightarrow{\text{2nd}} \Omega_s \xrightarrow[T_*]{\text{1st}} \Omega_h$$

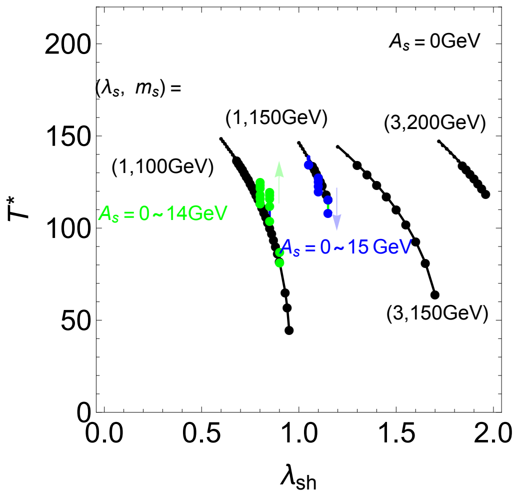

Two step PT (large A_s case)

$$\Omega_0 \xrightarrow[T_s^*]{\text{1st}} \Omega_s \xrightarrow[T_*]{\text{1st}} \Omega_h$$

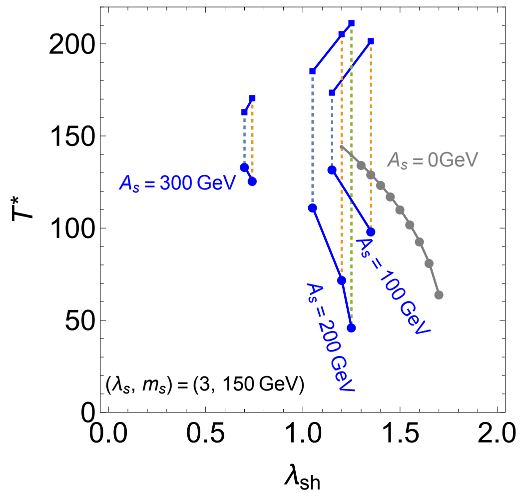

Three step PT

$$\Omega_0 \xrightarrow[T_s^*]{\text{1st}} \Omega_s \xrightarrow{\text{2nd}} \Omega_{sh} \xrightarrow[T_*]{\text{1st}} \Omega_h$$

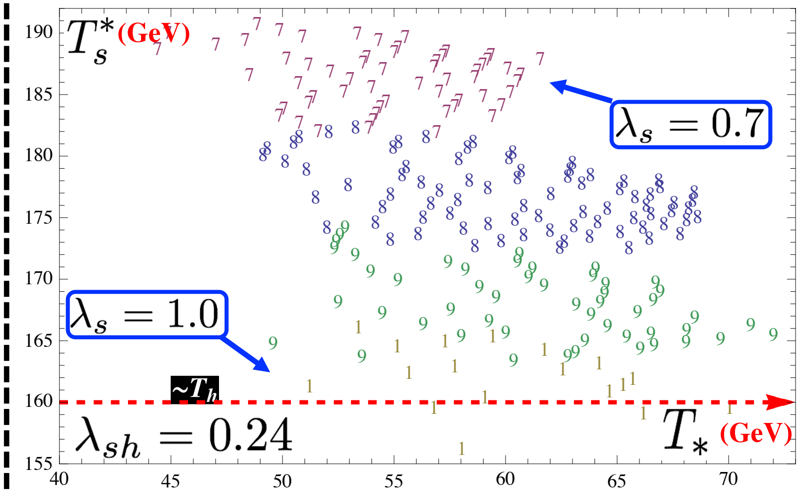

$$T_* \searrow \Longrightarrow \varphi_*/T_* \nearrow$$

Gravitational waves from 1stOPT

Two step PT (Z_2-like case)

$$\Omega_0 \xrightarrow{\text{2nd}} \Omega_s \xrightarrow[T_*]{\text{1st}} \Omega_h$$

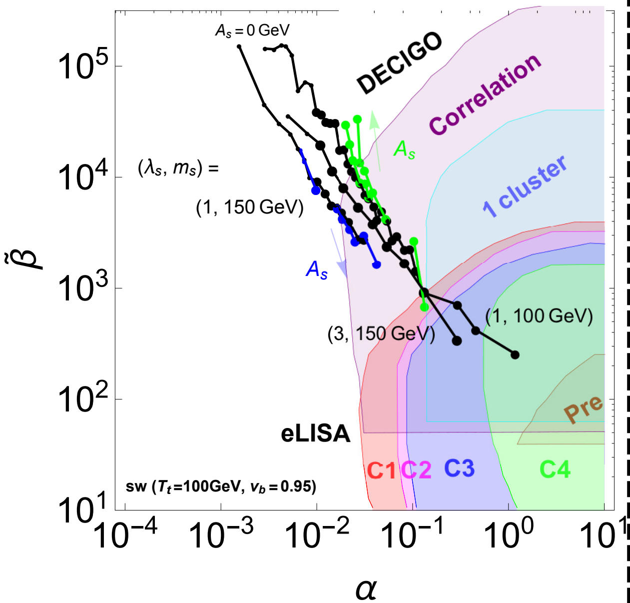

Two step PT (large A_s case)

$$\Omega_0 \xrightarrow[T_s^*]{\text{1st}} \Omega_s \xrightarrow[T_*]{\text{1st}} \Omega_h$$

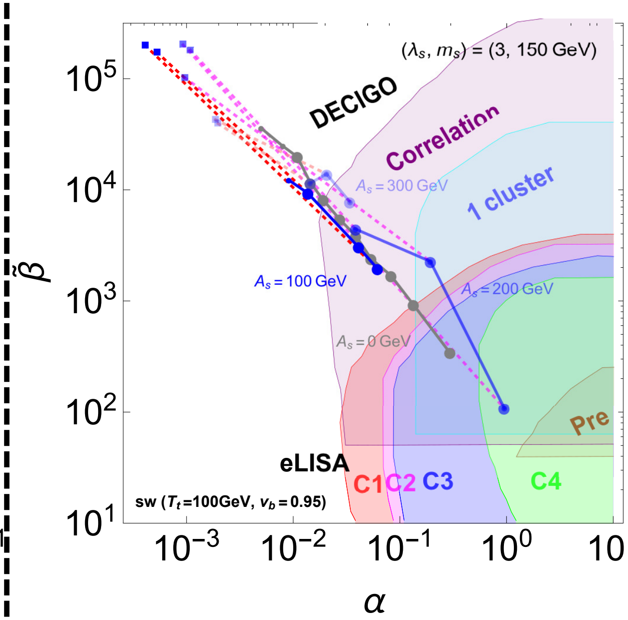

Three step PT

$$\Omega_0 \xrightarrow[T_s^*]{\text{1st}} \Omega_s \xrightarrow{\text{2nd}} \Omega_{sh} \xrightarrow[T_*]{\text{1st}} \Omega_h$$

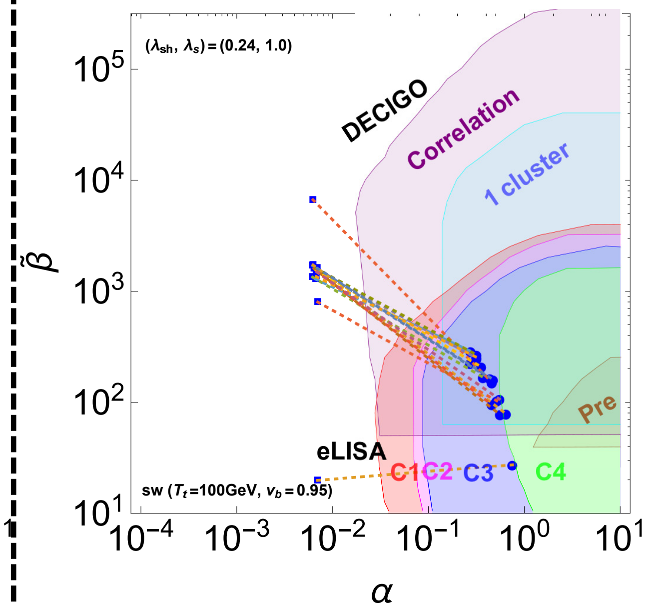

Sensitivities

- DECIGO [S.Kawamura, et al., Class. Quant. Grav. 28, 094011 (2011)]
- eLISA [C.Caprini *et al.*, arXiv:1512.06239 [astro-ph.CO]]

Conclusions

- The strongly 1stOPT can be realized by models with extended Higgs sector.
- Basically, these models can be tested at the colliders.

- However, there is another case: "nightmare scenario".
- In this talk, we have focused on a model with unbroken discrete symmetry.
- The potential barrier is created by "the multi-step PT" at finite temp.
- We have shown that, even if it is difficult to test at the colliders,
  - GW is significantly enhanced by the strongly 1stOPT
  - GW can be detected by future interferometers such as eLISA/DECIGO

Thank you for your attention!

Back Up

Dark Matter: Z_2-like case($A_s \rightarrow 0$)

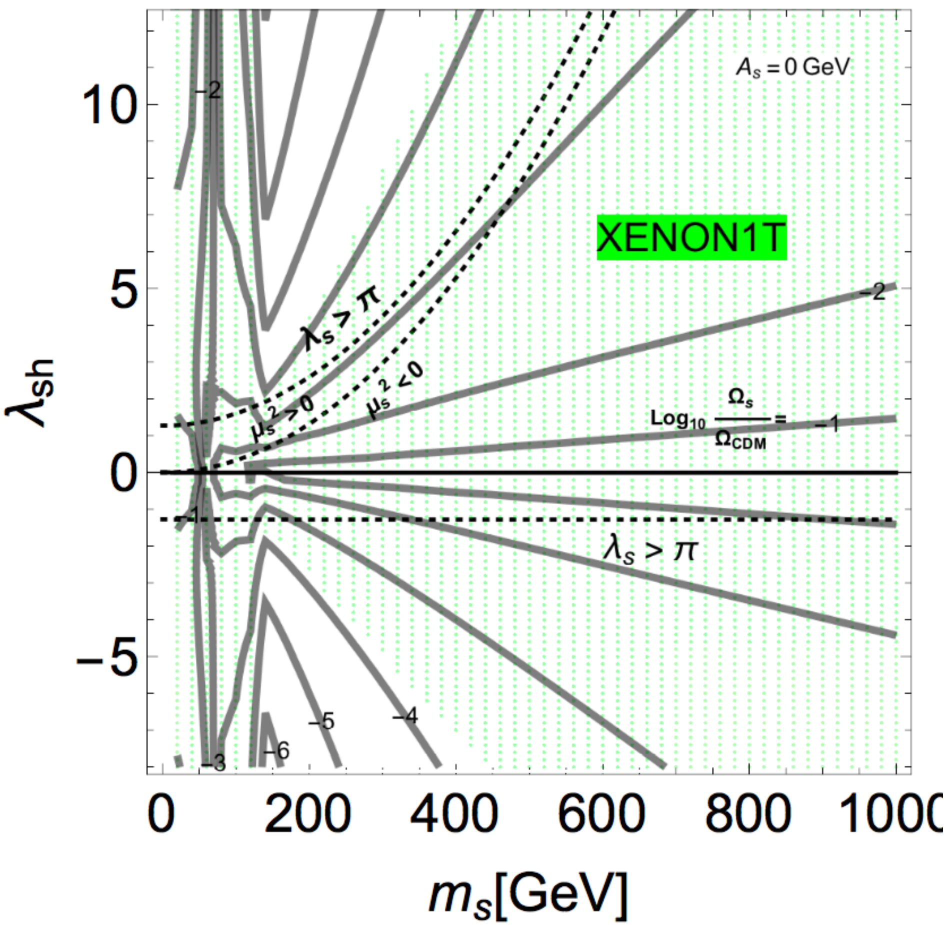

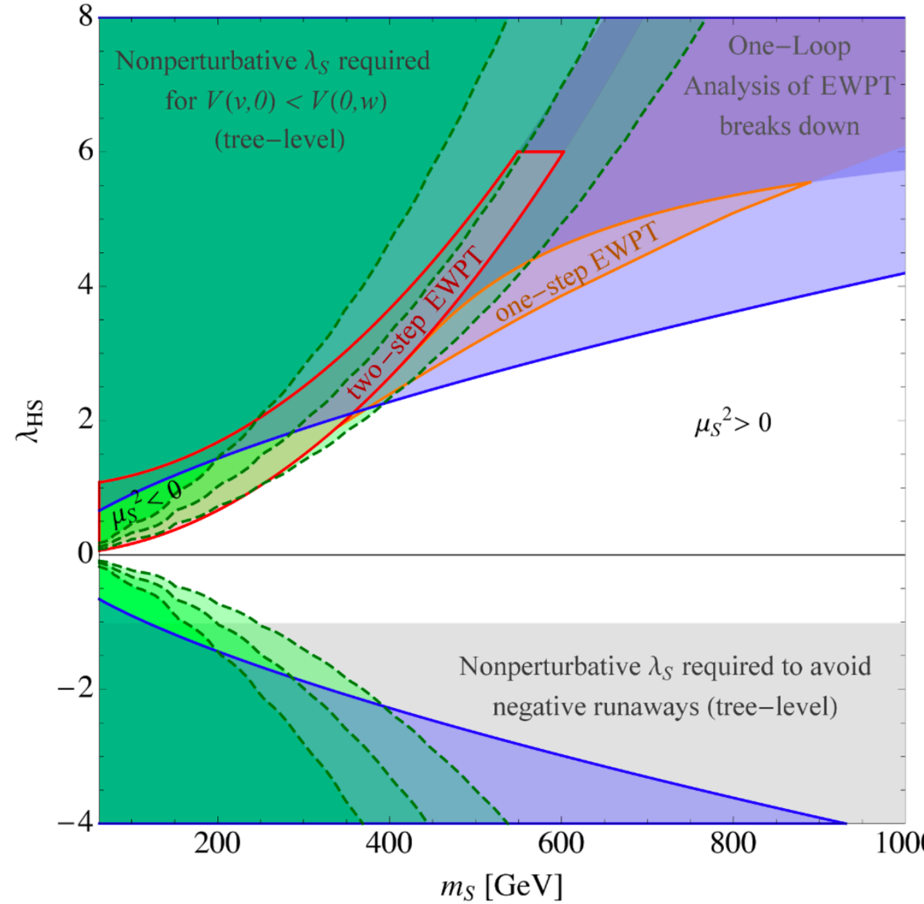

Curtin, Meade, Yu, 1409.0005

Dark Matter: finite A_s

100GeV

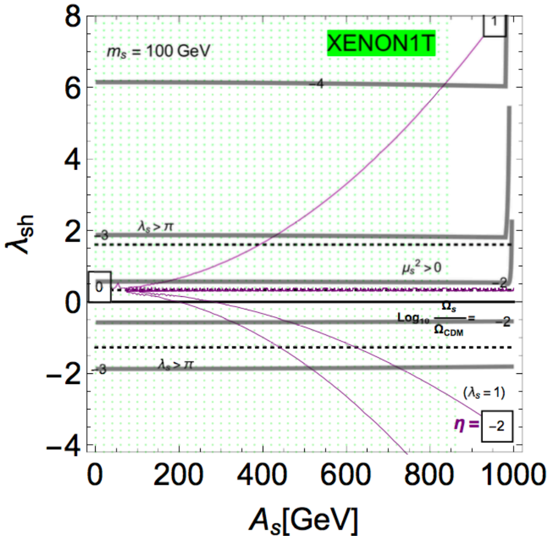

150GeV

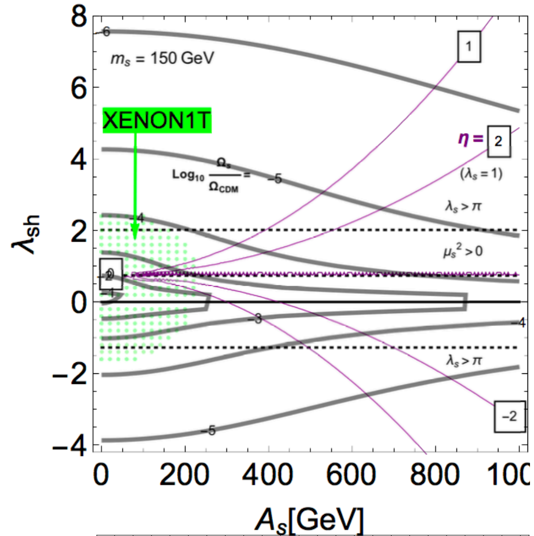

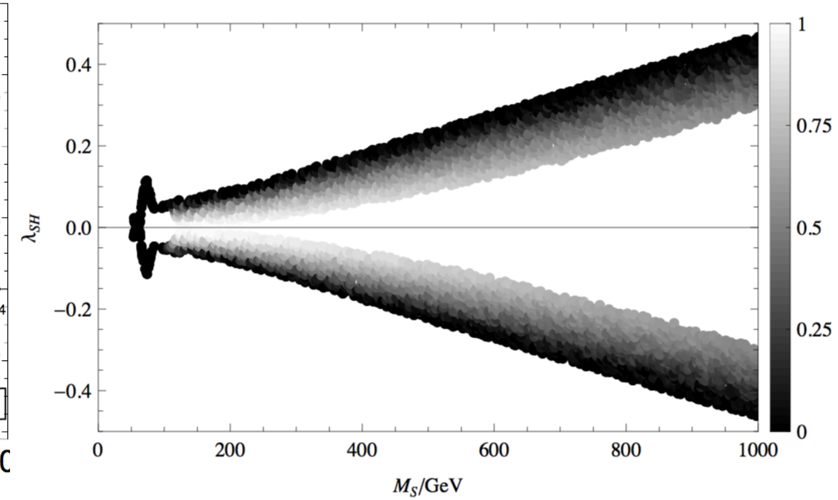

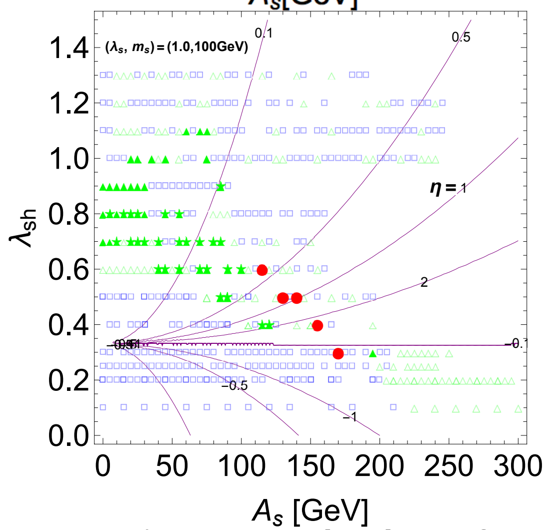

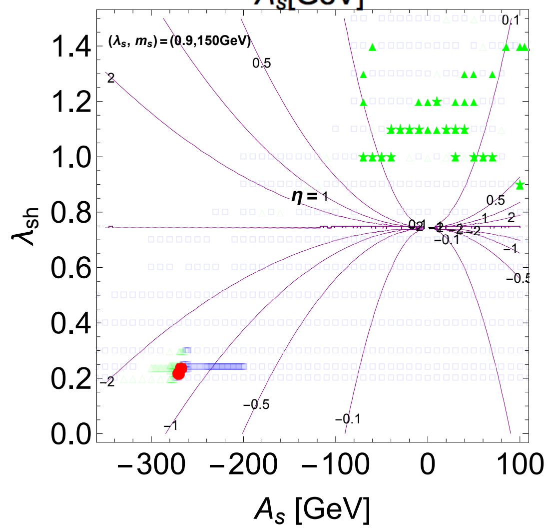

semi-annihilation is realized for small λ_{sh}

[Belanger, Kannike, Pukhovd, Raidal, 1211.1014]

However, the parameter regions which realize the strongly 1stOPT are not explained whole of the observed DM relic density.

Strongly 1stOPT and Higgs boson couplings

~ Probing the Higgs potential by "future colliders" ~

- Potential barrier by "Thermal loop effects"

The strength of phase transition

$$\boxed{\frac{\varphi_c}{T_c} = \frac{2E}{\lambda}\left(1 - \frac{e\lambda}{ET}\right)}$$

(analytic formula of couplings are given by one field & high-T approx.)

$$V_{\rm eff} = D(T^2 - T_0^2)\varphi^2 - (ET - e)\varphi^3 + \frac{\lambda(T)}{4}\varphi^4$$

e.g. Two Higgs doublet model (2HDM)

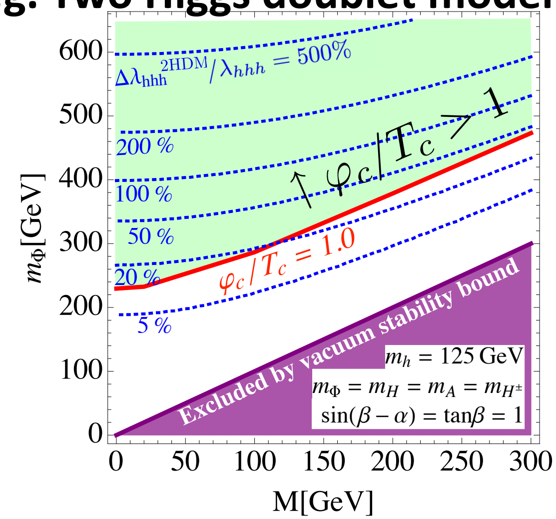

$$m_\Phi^2 \simeq M^2 + \lambda_i v^2 \quad \Phi = H, A, H^\pm$$

$$E = \frac{1}{12\pi v^3}\left\{6m_{W^\pm}^3 + 3m_Z^3 + \sum_\Phi m_\Phi^3 \left(1 - \frac{M^2}{m_\Phi^2}\right)^3 \left(1 + \frac{3}{2}\frac{M^2}{m_\Phi^2}\right)\right\}$$

$$\frac{\Delta\lambda_{hhh}}{\lambda_{hhh}} \equiv \frac{\lambda_{hhh} - \lambda_{hhh}^{\rm SM}}{\lambda_{hhh}^{\rm SM}}$$

Enhanced by $M \to 0$ limit (large λ_i)

$$\lambda_{hhh}^{\rm 2HDM} \equiv \frac{3m_h^2}{v}\left\{1 - \frac{m_t^4}{\pi^2 m_h^2 v^2} + \sum_\Phi \frac{m_\Phi^4}{12\pi^2 m_h^2 v^2}\left(1 - \frac{M^2}{m_\Phi^2}\right)^3\right\}$$

Kanemura, Okada, Senaha, PLB**606**, 361 (2005)

Large deviation in the *hhh* coupling is required! → EWPT can be tested at future colliders!

Strongly 1stOPT and Higgs boson couplings

～ Probing the Higgs potential by “future colliders” ～

- Potential barrier by **“Non-thermal tree level effects”**

$$\left(\frac{\varphi}{\sqrt{2}}, \varphi_S\right) \equiv (\bar{\varphi}\cos\alpha, \bar{\varphi}\sin\alpha)$$

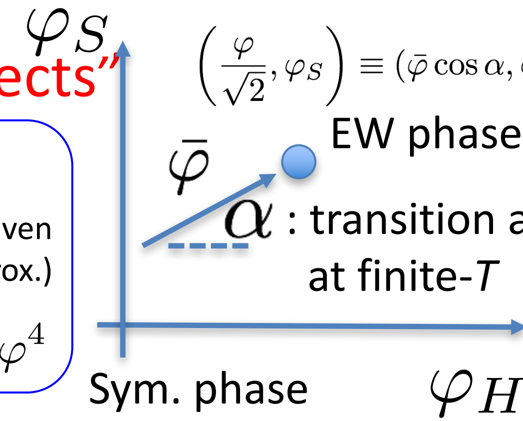

The strength of phase transition

$$\boxed{\frac{\varphi_c}{T_c} = \frac{2E}{\lambda}\left(1 - \frac{e\lambda}{ET}\right)}$$

(analytic formula of couplings are given by one field & high-T approx.)

$$V_{\mathrm{eff}} = D(T^2 - T_0^2)\varphi^2 - (ET - e)\varphi^3 + \frac{\lambda(T)}{4}\varphi^4$$

e.g. Higgs singlet model (HSM) ← cubic term is allowed

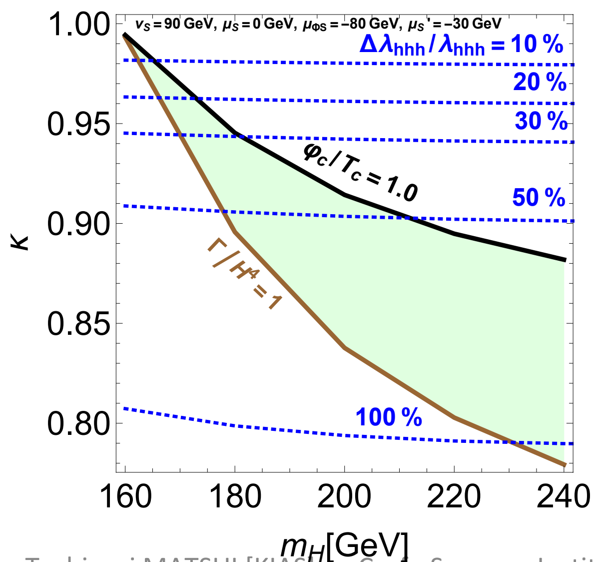

$$V_0 = -\mu_\Phi^2|\Phi|^2 + \lambda_\Phi|\Phi|^4 + \underline{\mu_{\Phi S}|\Phi|^2 S} + \frac{\lambda_{\Phi S}}{2}|\Phi|^2 S^2 + \mu_S^3 S + \frac{m_S^2}{2}S^2 + \underline{\frac{\mu_S'}{3}S^3} + \frac{\lambda_S}{4}S^4$$

$$\boxed{e = \left(\mu_{\Phi S}\cos^2\alpha + \frac{\mu_S'}{3}\sin^2\alpha\right)\sin\alpha} \quad <0$$

$$\boxed{\frac{\Delta\lambda_{hhh}}{\lambda_{hhh}} \equiv \frac{\lambda_{hhh} - \lambda_{hhh}^{\mathrm{SM}}}{\lambda_{hhh}^{\mathrm{SM}}}}$$

θ : mixing angle at zero-T

$$\boxed{\lambda_{hhh}^{\mathrm{HSM,tree}} = 6\left(\lambda_\Phi v_\Phi c_\theta^3 + \frac{\mu_{\Phi S}}{2}s_\theta c_\theta^2 + \frac{\lambda_{\Phi S}}{2}s_\theta c_\theta(v_\Phi s_\theta + v_S c_\theta) + \left(\frac{\mu_S'}{3} + \lambda_S v_S\right)s_\theta^3\right)}$$

$$\boxed{\kappa_i \equiv g_{hii}/g_{hii}^{\mathrm{SM}}} \qquad \boxed{\kappa \equiv \kappa_V = \kappa_F = \cos\theta}$$

Fuyuto, Senaha, PRD **90**, no. 1, 015015 (2014)

Models of 1stOPT

Higgs potential by high temperature approximation

$$V_{\rm eff} = D(T^2 - T_0^2)\varphi^2 - (ET - e)\varphi^3 + \frac{\lambda(T)}{4}\varphi^4 \Rightarrow \frac{\varphi_c}{T_c} = \frac{2E}{\lambda}\left(1 - \frac{e\lambda}{ET}\right)$$

- *E* : thermal coupling (the non-decoupling effects due to the additional boson loop)
- *−e* : non-thermal coupling (the field mixing of the Higgs boson with additional scalar fields)

J. Kehayias and S. Profumo, JCAP**1003**, 003 (2010)

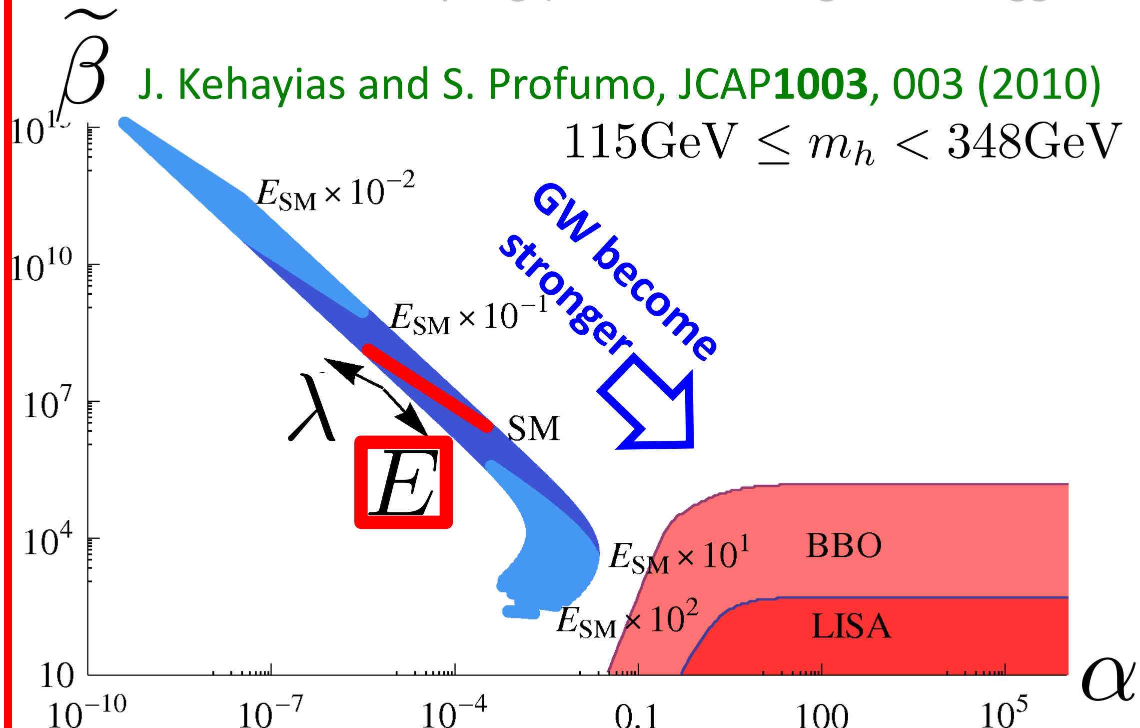

As the simplest model, we have investigated **the O(N) model**.

Kakizaki, Kanemura, TM, PRD **92**, 115007 (2015);
Hashino, Kakizaki, Kanemura, TM, PRD **94**, 015005 (2016)

Models of 1stOPT

Higgs potential by high temperature approximation

$$V_{\text{eff}} = D(T^2 - T_0^2)\varphi^2 - (ET - e)\varphi^3 + \frac{\lambda(T)}{4}\varphi^4 \Rightarrow \boxed{\frac{\varphi_c}{T_c} = \frac{2E}{\lambda}\left(1 - \frac{e\lambda}{ET}\right)}$$

- E : thermal coupling (the non-decoupling effects due to the additional boson loop)
- $-e$: non-thermal coupling (the field mixing of the Higgs boson with additional scalar fields)

J. Kehayias and S. Profumo, JCAP**1003**, 003 (2010)

$$115\text{GeV} \leq m_h < 348\text{GeV}$$

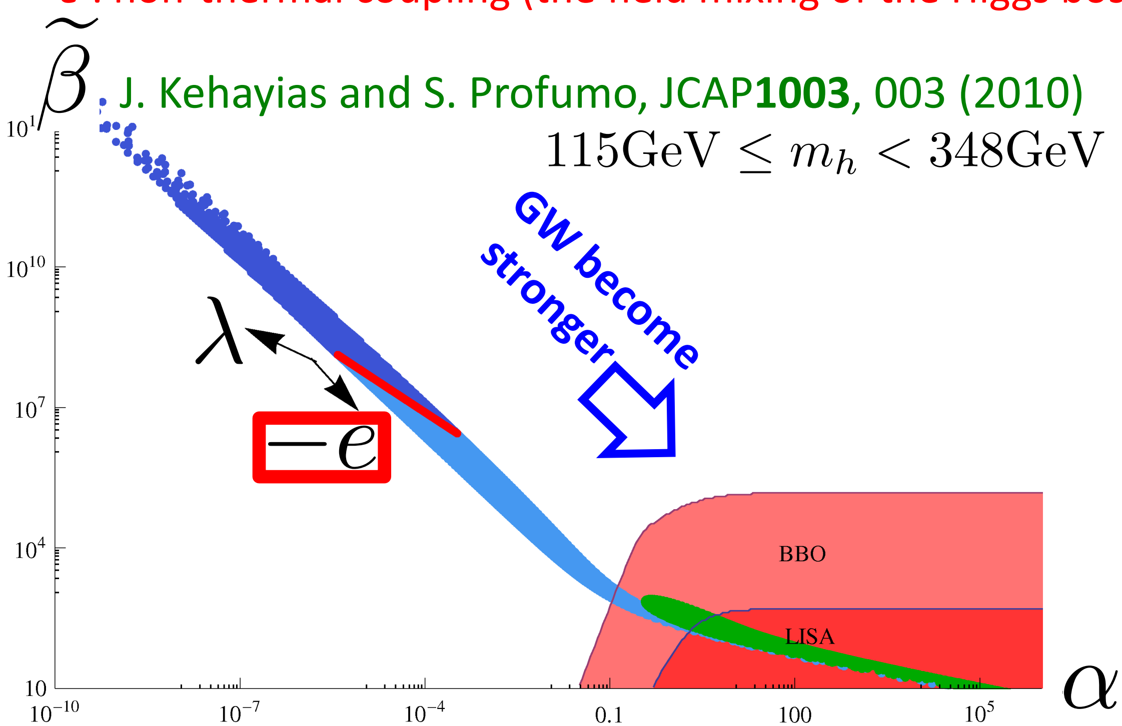

As the simplest model, we have investigated **the Higgs singlet model**.

Hashino, Kakizaki, Kanemura, TM, Ko, PLB **766**, 49 (2017)

Strongly 1st OPT and Higgs boson couplings

~ Probing the Higgs potential by "future colliders" ~

- Deviation of Higgs couplings from SM: $\kappa_i \equiv g_{hii}/g_{hii}^{\mathrm{SM}}$
  - Recent LHC data: $\boxed{\kappa_Z = 1.03^{+0.11}_{-0.11}, \kappa_W = 0.91^{+0.10}_{-0.10}}$

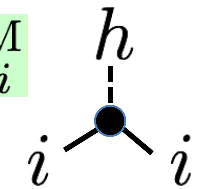

    (1σ; combination of ATLAS and CMS) [ATLAS-CONF-2015-044]
  - Expected accuracy: κ_V : 2%@HL-LHC 14TeV 3000fb^{-1} [CMS collaboration, 1307.7135],
    κ_V : 0.6% @ILC 250GeV 2000fb^{-1} [Durieux et al. (2017)]
    κ_Z (κ_W) : 0.37% (0.51%) @ILC 500GeV 500fb^{-1} [Fujii et al, 1506.05992]
- Deviation of *hhh* coupling from SM: $\Delta\lambda_{hhh} \equiv \dfrac{\lambda_{hhh}^{\mathrm{HSM}} - \lambda_{hhh}^{\mathrm{SM}}}{\lambda_{hhh}^{\mathrm{SM}}}$
  - Expected accuracy: 54%@HL-LHC 14TeV 3000fb^{-1} [CMS-PAS-FTR-15-002],
    27%@ILC 500GeV 4000fb^{-1} [Fujii et al, 1506.05992],
    16% (10%)@ILC 1TeV 2000fb^{-1} (5000fb^{-1}) [Fujii et al, 1506.05992]
- In order to explore EWPT, synergy between the measurements of various Higgs boson couplings at future collider experiments and the observation of GWs at future space-based interferometers can be useful to determine model parameters [Kakizaki, Kanemura, TM (PRD'15); Hashino, Kakizaki, Kanemura, TM (PRD'16); Hashino, Kakizaki, Kanemura, TM, Ko, (PLB'17)]

Gravitational wave observations

eLISA design decided

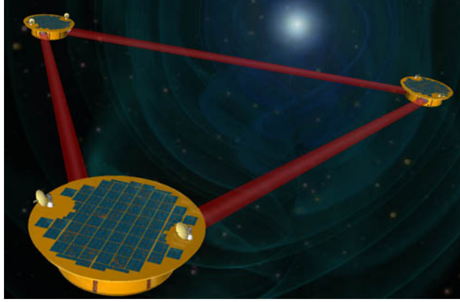

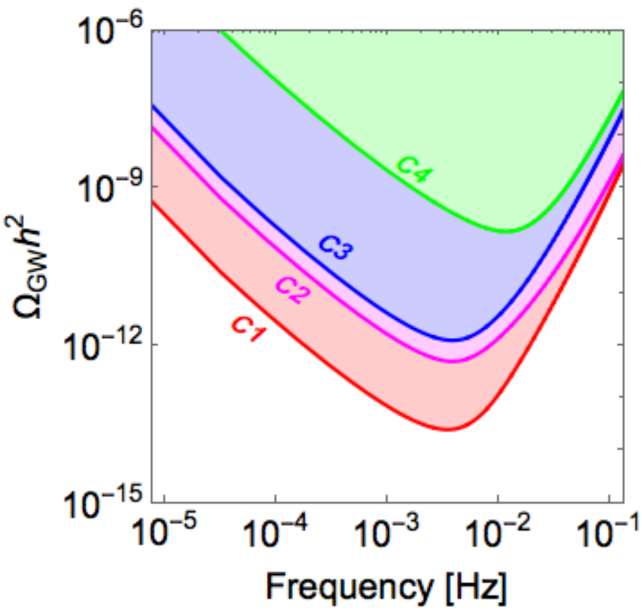

Properties of the representative eLISA configurations

Name	C1	C2	C3	C4
Full name	N2A5M5L6	N2A1M5L6	N2A2M5L4	N1A1M2L4
# links	6	6	4	4
Arm length [km]	5M	1M	2M	1M
Duration [years]	5	5	5	2
Noise level	N2	N2	N2	N1

eLISA cosmology WG report, arXiv:1512.06239 [JCAP(2016)]

C1 : old LISA configuration

- **Number of laser links : 6**, corresponding to **3** interferometer arms
  → Determined at eLISA symposium (Sept. 2016, U. of Zurich) http://www.physik.uzh.ch/events/lisa2016
- **Arm length : 2 - 5** million km
- **Duration : 3 - 10** years data taking

} Extra budget was estimated

- **Noise level** : **N2** (LISA pathfinder expected) is 10 times larger than N1 (LISA pathfinder required)
  → Determined by receiving the pathfinder result [PRL**116**, 231101 (2016)]

ESA approval : **June, 2017**
Launch : **2034**

LIGO have detected GWs

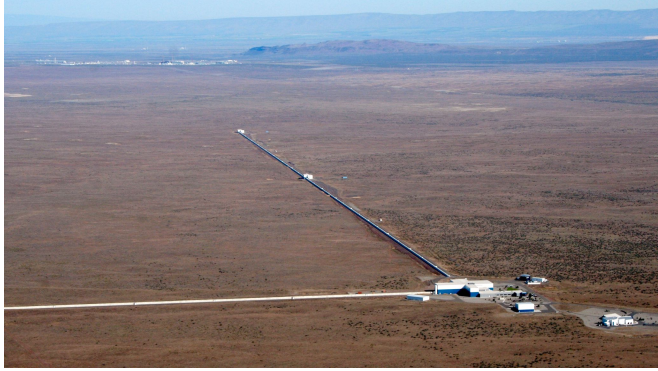

- “GW150914” LIGO Scientific and Virgo Collaborations, Phys. Rev. Lett. **116**, no. 6, 061102 (2016)
  - BH merger (36+29→62 in the unit of solar mass)
  - 410Mpc (1.3 billion years ago)
  - Signal/Noise=24 (>5.1σ), frequency: 35-250 Hz
- "GW151226” LIGO Scientific and Virgo Collaborations, Phys. Rev. Lett. **116**, no. 24, 241103 (2016)
  - BH merger (14+8→21 in the unit of solar mass)
  - 440Mpc (1.4 billion years ago)
  - Signal/Noise=13 (>5σ), frequency: 35-450 Hz,

Prospects for LIGO/Virgo

- LIGO 1st RUN (2015/09/12-2016/01/19)
- LIGO 2nd RUN (from the fall 2016)
  - 15-25% improvement in sensitivity performance over 1st RUN
  - The event rate will be increased by 1.5-2 times

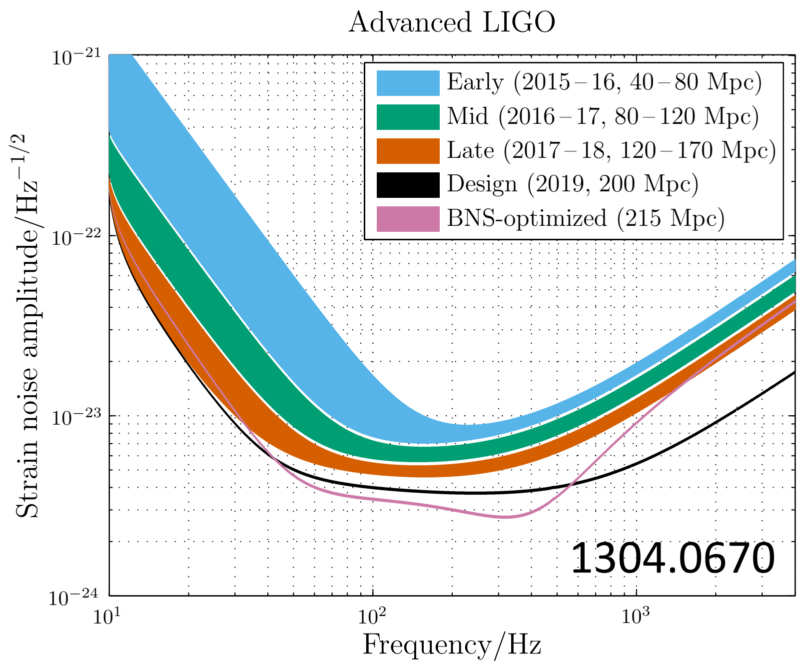

Observing run	Epoch	Duration (months)	aLIGO sensitivity	AdVirgo sensitivity
O1	2015–2016	4	Early	—
O2	2016–2017	6	Mid	Early
O3	2017–2018	9	Late	Mid
O4	2019	12	Design	Late
O5	2020+	–	Design	Design

1602.03847

Pulsar Timing Array

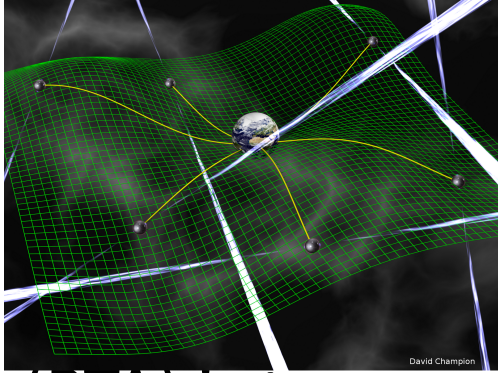

- The main idea behind pulsar timing array (PTA) is to use ultra-stable millisecond pulsars as beacons for detecting GW in the nano-Hz range (10^{-9} – 10^{-7} Hz).
- Pulsars are neutron stars with rapid rotation and strong magnetic field. Period from few seconds to few milliseconds.

Pulsar Timing Array

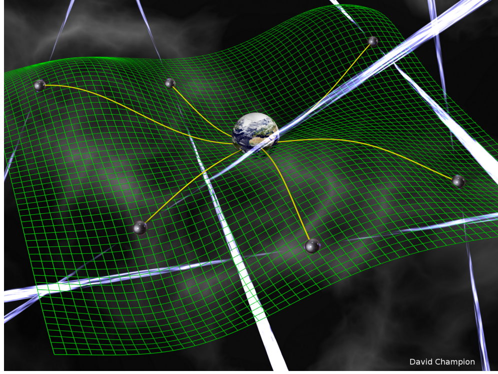

- Current limit: $\Omega_{GW}h^2 >\sim 10^{-9}$

  EPTA Collaboration [Mon. Not. Roy. Astron. Soc. **453**, no. 3, 2576 (2015) [arXiv:1504.03692]]

  NANOGrav Collaboration [Astrophys. J. **821**, no. 1, 13 (2016) [arXiv:1508.03024]]

- **International Pulsar Timing Array** (IPTA): combined three PTAs [PPTA (Australian), EPTA (European)*, NanoGrav (North American)]. *EPTA consists of 5 radio telescopes

  1st data release Mon. Not. Roy. Astron. Soc. **458**, 1267 (2016) [arXiv:1602.03640]

  Expected limit: $\Omega_{GW}h^2 >\sim 10^{-12}$ Publ. Astron. Soc. Austral. **30**, 17 (2013) [arXiv:1210.6130]

- **Square Kilometer Array** (SKA)

  : The next great advancement in radio astronomy

  Expected limit: $\Omega_{GW}h^2 >\sim 10^{-15}$ https://www.skatelescope.org

Gravitational wave from 1^{st} order phase transition

GWs from 1stOPT

C. Caprini *et al.*, JCAP**1604**, 001 (2016)

Expanding bubbles of the broken phase

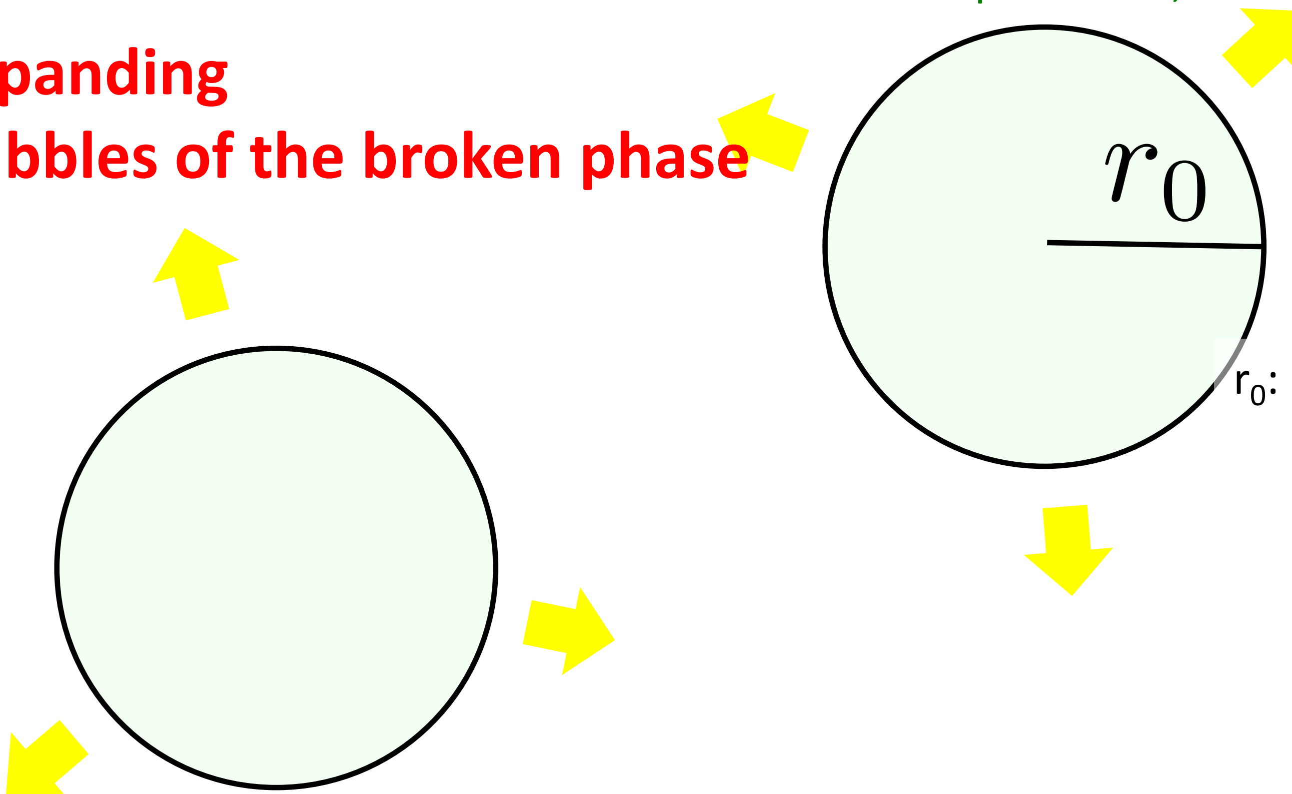

r_0: size of critical bubble

Bubble is spherical

No GW occurs

GWs from 1stOPT

C. Caprini *et al.*, JCAP**1604**, 001 (2016)

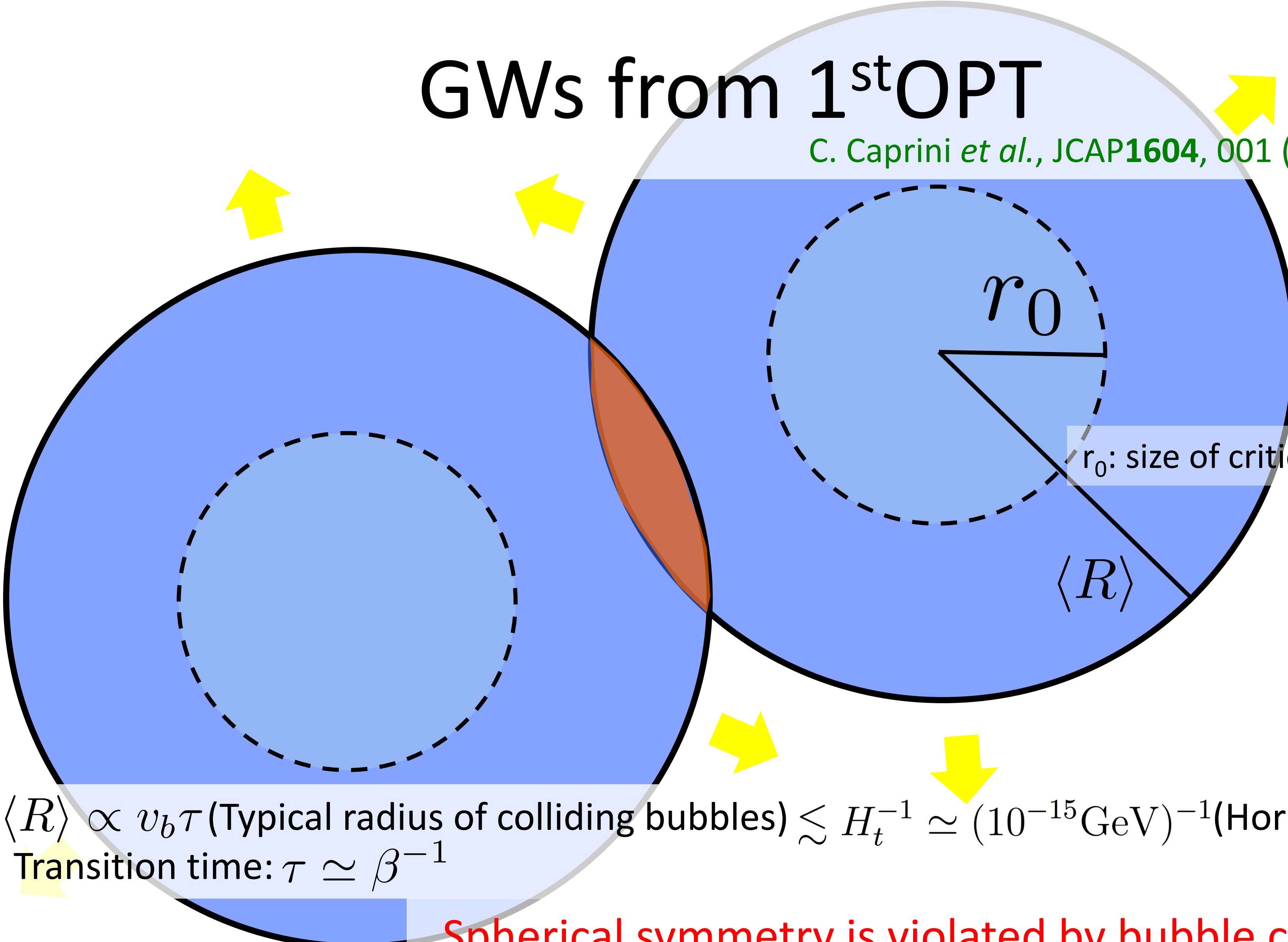

$\langle R \rangle \propto v_b \tau$ (Typical radius of colliding bubbles) $\lesssim H_t^{-1} \simeq (10^{-15}\mathrm{GeV})^{-1}$ (Horizon size),
Transition time: $\tau \simeq \beta^{-1}$

Spherical symmetry is violated by bubble collisions

GWs from 1^{st}OPT

C. Caprini *et al.*, JCAP**1604**, 001 (2016)

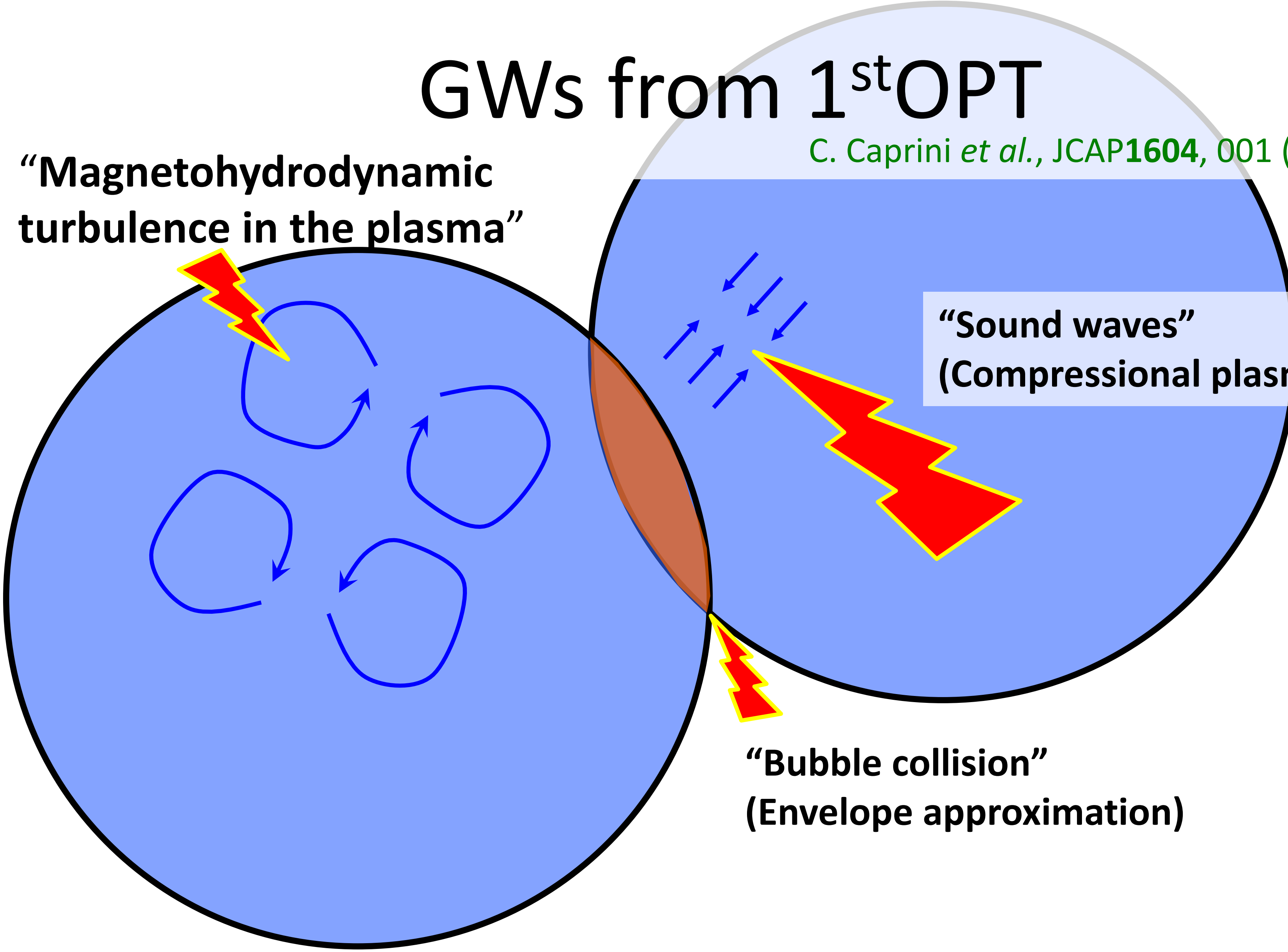

Relic abundance of GWs

Model parameters

(*) C. Caprini *et al.*, JCAP**1604**, 001 (2016)

Input

$$V_{\rm eff}(\varphi, T) \longrightarrow \alpha,\ \tilde{\beta} \xrightarrow{\text{Prediction}^*} \Omega_{\rm GW}(f)h^2$$

@T=T$_t$

(Observable)

Relic abundance of GWs @ peak frequency

$$\widetilde{\Omega}_{\rm sw}h^2 \simeq 2.65\times10^{-6}\frac{v_b}{\tilde{\beta}}\left(\frac{\kappa(v_b,\alpha)\alpha}{1+\alpha}\right)^2 \quad @\ \tilde{f}_{\rm sw} \simeq 1.9\times10^{-5}\ {\rm Hz}\frac{\widetilde{\beta}(T_t/100\ {\rm GeV})}{v_b}$$

$$\widetilde{\Omega}_{\rm env}h^2 \simeq \frac{1.84\times10^{-6}v_b^3}{(0.42+v_b^2)\tilde{\beta}^2}\left(\frac{\kappa(v_b,\alpha)\alpha}{1+\alpha}\right)^2 \quad @\ \tilde{f}_{\rm env} \simeq 1.0\times10^{-5}\ {\rm Hz}\frac{\widetilde{\beta}(T_t/100\ {\rm GeV})}{1.8-0.1v_b+v_b^2}$$

$$\widetilde{\Omega}_{\rm turb}h^2 \simeq \frac{9.35\times10^{-8}v_b^2}{0.00354v_b\tilde{\beta}+\tilde{\beta}^2}\left(\frac{\epsilon\kappa(v_b,\alpha)\alpha}{1+\alpha}\right)^{3/2} \quad @\ \tilde{f}_{\rm turb} \simeq 2.7\times10^{-5}\ {\rm Hz}\frac{\widetilde{\beta}(T_t/100\ {\rm GeV})}{v_b}$$

Estimation of the relic abundance

M. Kamionkowski, PRD**49**, 2837 (1994)

- Wave eq. from Einstein eq. in weak field approximation

$$-\Box\left(h_{\mu\nu}-\frac{1}{2}\eta_{\mu\nu}h^{\alpha}{}_{\alpha}\right)=16\pi G T_{\mu\nu}$$

$$\begin{cases} T^0_0 = \rho_{\rm kin} + \cdots \\ \dfrac{d}{dt} \simeq \beta \end{cases}$$

- Stochastic backgrounds of GWs

$$\rho_{\rm GW}=\frac{1}{32\pi G} < \dot{h}_{\alpha\beta}\dot{h}^{\alpha\beta} > \sim \underline{8\pi G\rho_{\rm kin}^2/\beta^2}$$

$$\underline{\rho_{\rm tot}(=\underbrace{\rho_{\rm vac}}_{(=\epsilon)}+\rho_{\rm rad})=\frac{3H^2}{8\pi G}} \qquad \alpha=\frac{\rho_{\rm vac}}{\rho_{\rm rad}} \qquad \kappa=\frac{\rho_{\rm kin}}{\rho_{\rm vac}}$$

Efficiency factor

$$\Omega_{\rm GW}=\frac{\rho_{GW}}{\rho_{\rm tot}}\simeq\underbrace{\left(\frac{H}{\beta}\right)^2}_{=\widetilde{\beta}^{-2}\sim(H\langle R\rangle)^2}\left(\frac{\kappa\alpha}{1+\alpha}\right)^2$$

Origins of GWs from EWPT

C. Caprini *et al.*, arXiv:1512.06239 [astro-ph.CO] (review)

2.1 Contributions to the Gravitational Wave Spectrum

To varying degrees, three processes are involved in the production of GWs at a first-order PT:

- Collisions of bubble walls and (where relevant) shocks in the plasma. This can be treated by a technique now generally referred to as the 'envelope approximation' [10–15]. As described below, this approximation can be used to compute the contribution to the GW spectrum from the scalar field, ϕ, itself.
- Sound waves in the plasma after the bubbles have collided but before expansion has dissipated the kinetic energy in the plasma [16–19].
- Magnetohydrodynamic (MHD) turbulence in the plasma forming after the bubbles have collided [20–25].

We improve our analysis in accordance with the recent simulation result.

Recent work of other souse of GW "sound wave"

M. Hindmarsh, *et al.*, PRL **112**, 041301 (2014); arXiv:1504.03291 [astro-ph.CO].

Numerical simulations of acoustically generated gravitational waves at a first order phase transition

Mark Hindmarsh,[1,2,*] Stephan J. Huber,[1,†] Kari Rummukainen,[2,‡] and David J. Weir[3,§]

[1] *Department of Physics and Astronomy, University of Sussex, Falmer, Brighton BN1 9QH, U.K.*
[2] *Department of Physics and Helsinki Institute of Physics, PL 64, FI-00014 University of Helsinki, Finland*
[3] *Institute of Mathematics and Natural Sciences, University of Stavanger, 4036 Stavanger, Norway*

(Dated: April 14, 2015)

We present details of numerical simulations of the gravitational radiation produced by a first order thermal phase transition in the early universe. We confirm that the dominant source of gravitational waves is sound waves generated by the expanding bubbles of the low-temperature phase. We demonstrate that the sound waves have a power spectrum with power-law form between the scales set by the average bubble separation (which sets the length scale of the fluid flow L_{f}) and the bubble wall width. The sound waves generate gravitational waves whose power spectrum also has a power-law form, at a rate proportional to L_{f} and the square of the fluid kinetic energy density. We identify a dimensionless parameter $\tilde{\Omega}_{\mathrm{GW}}$ characterising the efficiency of this "acoustic" gravitational wave production whose value is $8\pi\tilde{\Omega}_{\mathrm{GW}} \simeq 0.8 \pm 0.1$ across all our simulations. <u>We compare the acoustic gravitational waves with the standard prediction from the envelope approximation</u>. Not only is the power spectrum steeper (apart from an initial transient) but <u>the gravitational wave energy density is generically two orders of magnitude or more larger</u>.

Origins of GWs from EWPT

C. Caprini *et al.*, arXiv:1512.06239 [astro-ph.CO] (review)

- Vacuum bubble velocity v_b

- Efficiency factor $\kappa(v_b, \alpha)$

$$\widetilde{\Omega}_{\rm sw} h^2 \simeq 2.65 \times 10^{-6} \frac{v_b}{\tilde{\beta}} \left(\frac{\kappa(v_b, \alpha)\alpha}{1+\alpha} \right)^2 \quad @ \quad \tilde{f}_{\rm sw} \simeq 1.9 \times 10^{-5} {\rm Hz} \frac{\tilde{\beta}}{v_b}$$

$$\widetilde{\Omega}_{\rm env} h^2 \simeq \frac{1.84 \times 10^{-6} v_b^3}{(0.42 + v_b^2)\tilde{\beta}^2} \left(\frac{\kappa(v_b, \alpha)\alpha}{1+\alpha} \right)^2 \quad @ \quad \tilde{f}_{\rm env} \simeq 1.0 \times 10^{-5} {\rm Hz} \frac{\tilde{\beta}}{1.8 - 0.1 v_b + v_b^2}$$

$$\widetilde{\Omega}_{\rm turb} h^2 \simeq \frac{9.35 \times 10^{-8} v_b^2}{0.00354 v_b \tilde{\beta} + \tilde{\beta}^2} \left(\frac{\epsilon\kappa(v_b, \alpha)\alpha}{1+\alpha} \right)^{3/2} \quad @ \quad \tilde{f}_{\rm turn} \simeq 2.7 \times 10^{-5} {\rm Hz} \frac{\tilde{\beta}}{v_b}$$

Origins of GWs from EWPT

C. Caprini *et al.*, arXiv:1512.06239 [astro-ph.CO] (review)

- Vacuum bubble velocity v_b

- Efficiency factor $\kappa(v_b , \alpha)$

$$\kappa(v_b, \alpha) \simeq O(0.01 - 0.1)$$

J.R.Espinosa, *et al*, JCAP **1006**, 028 (2010)

$$\widetilde{\Omega}_{\rm sw} h^2 \simeq 2.65 \times 10^{-6} \frac{v_b}{\tilde{\beta}} \left(\frac{\kappa(v_b, \alpha) \alpha}{1+\alpha} \right)^2 \quad @ \ \tilde{f}_{\rm sw} \simeq 1.9 \times 10^{-5} {\rm Hz} \frac{\tilde{\beta}}{v_b}$$

$$\widetilde{\Omega}_{\rm env} h^2 \simeq \frac{1.84 \times 10^{-6} v_b^3}{(0.42 + v_b^2) \tilde{\beta}^2} \left(\frac{\kappa(v_b, \alpha) \alpha}{1+\alpha} \right)^2 \quad @ \ \tilde{f}_{\rm env} \simeq 1.0 \times 10^{-5} {\rm Hz} \frac{\tilde{\beta}}{1.8 - 0.1 v_b + v_b^2}$$

$$\widetilde{\Omega}_{\rm turb} h^2 \simeq \frac{9.35 \times 10^{-8} v_b^2}{0.00354 v_b \tilde{\beta} + \tilde{\beta}^2} \left(\frac{\epsilon \kappa(v_b, \alpha) \alpha}{1+\alpha} \right)^{3/2} \quad @ \ \tilde{f}_{\rm turn} \simeq 2.7 \times 10^{-5} {\rm Hz} \frac{\tilde{\beta}}{v_b}$$

Origins of GWs from EWPT

C. Caprini *et al.*, arXiv:1512.06239 [astro-ph.CO] (review)

- Vacuum bubble velocity v_b
- Efficiency factor $\kappa(v_b, \alpha)$

$$\kappa(v_b, \alpha) \simeq O(0.01 - 0.1)$$

J.R.Espinosa, *et al*, JCAP **1006**, 028 (2010)

- The fraction of bulk motion from the bubble walls

The result from resent simulation

$$\epsilon \simeq 0.05 - 0.10$$

Hindmarsh, Huber, Rummukainen, Weir, PRD **92**, no. 12, 123009 (2015)

$$\widetilde{\Omega}_{\rm sw} h^2 \simeq 2.65 \times 10^{-6} \frac{v_b}{\tilde{\beta}} \left(\frac{\kappa(v_b, \alpha)\alpha}{1+\alpha} \right)^2 \quad @ \ \tilde{f}_{\rm sw} \simeq 1.9 \times 10^{-5} {\rm Hz} \frac{\tilde{\beta}}{v_b}$$

$$\widetilde{\Omega}_{\rm env} h^2 \simeq \frac{1.84 \times 10^{-6} v_b^3}{(0.42 + v_b^2)\tilde{\beta}^2} \left(\frac{\kappa(v_b, \alpha)\alpha}{1+\alpha} \right)^2 \quad @ \ \tilde{f}_{\rm env} \simeq 1.0 \times 10^{-5} {\rm Hz} \frac{\tilde{\beta}}{1.8 - 0.1 v_b + v_b^2}$$

$$\widetilde{\Omega}_{\rm turb} h^2 \simeq \frac{9.35 \times 10^{-8} v_b^2}{0.00354 v_b \tilde{\beta} + \tilde{\beta}^2} \left(\frac{\epsilon\kappa(v_b, \alpha)\alpha}{1+\alpha} \right)^{3/2} \quad @ \ \tilde{f}_{\rm turn} \simeq 2.7 \times 10^{-5} {\rm Hz} \frac{\tilde{\beta}}{v_b}$$

(α, βtilde) ⇔ (f, $\Omega_{GW}h^2$)$_{new}$

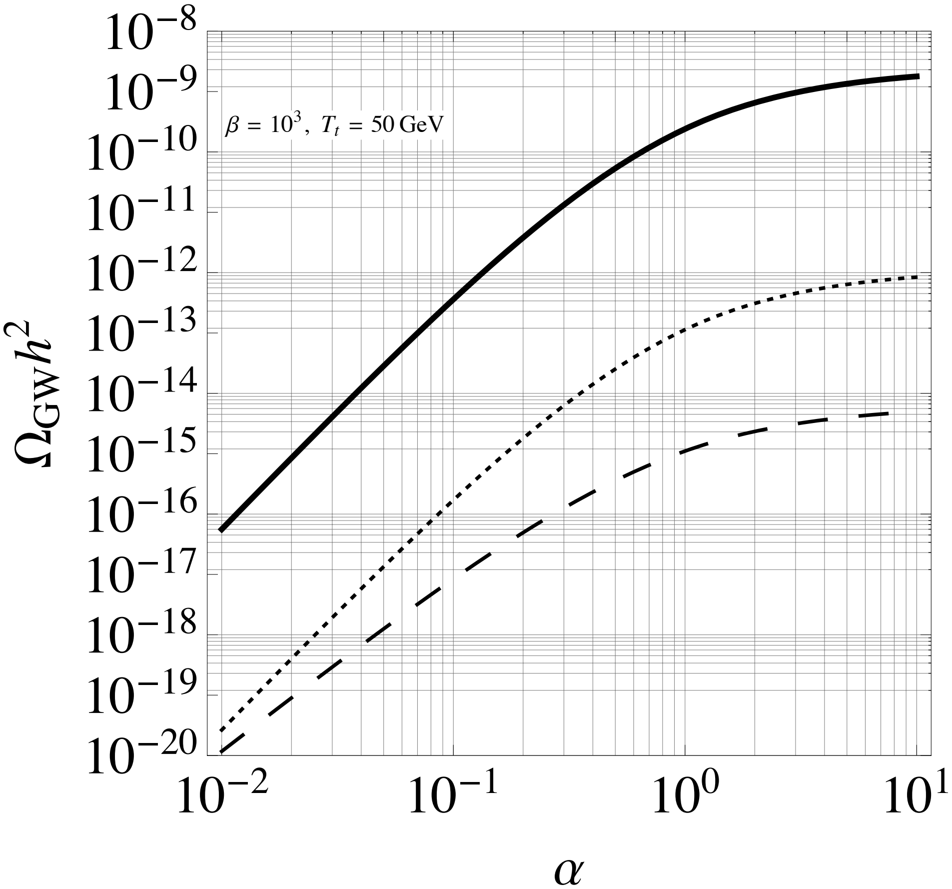

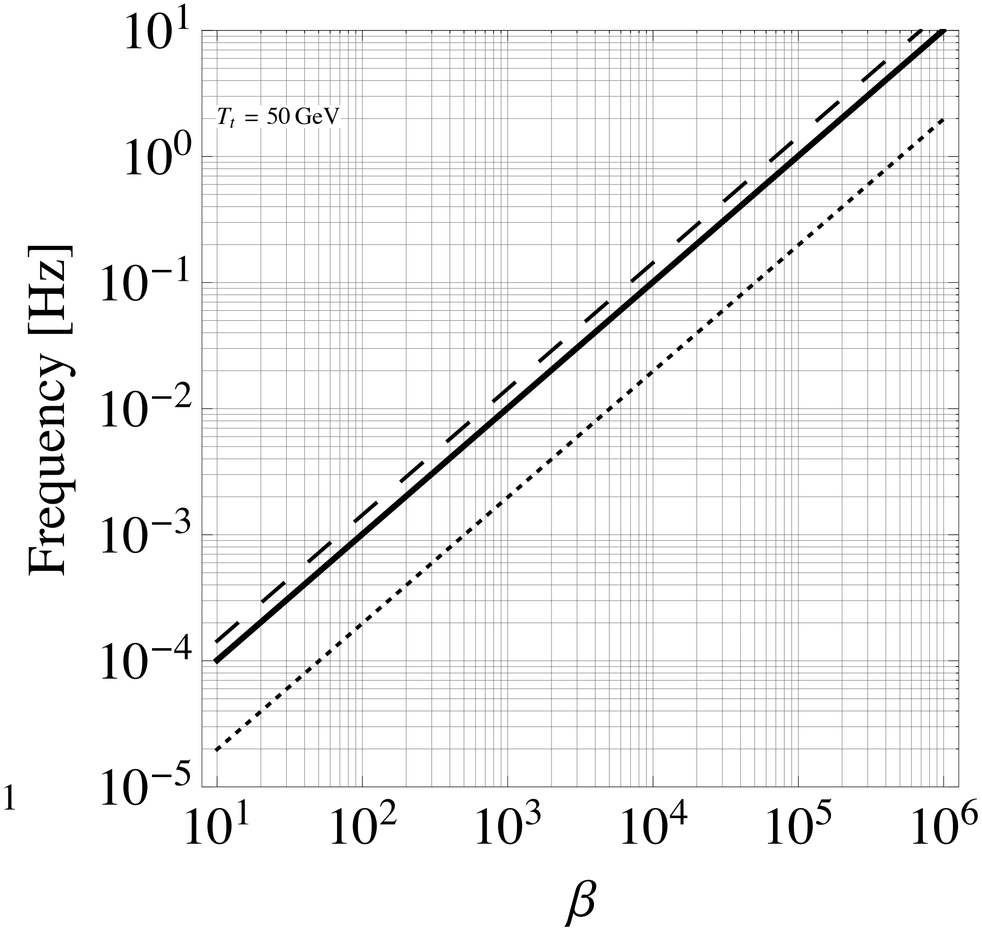

(α, βtilde)_exp. by New spectra (T_t=50GeV)

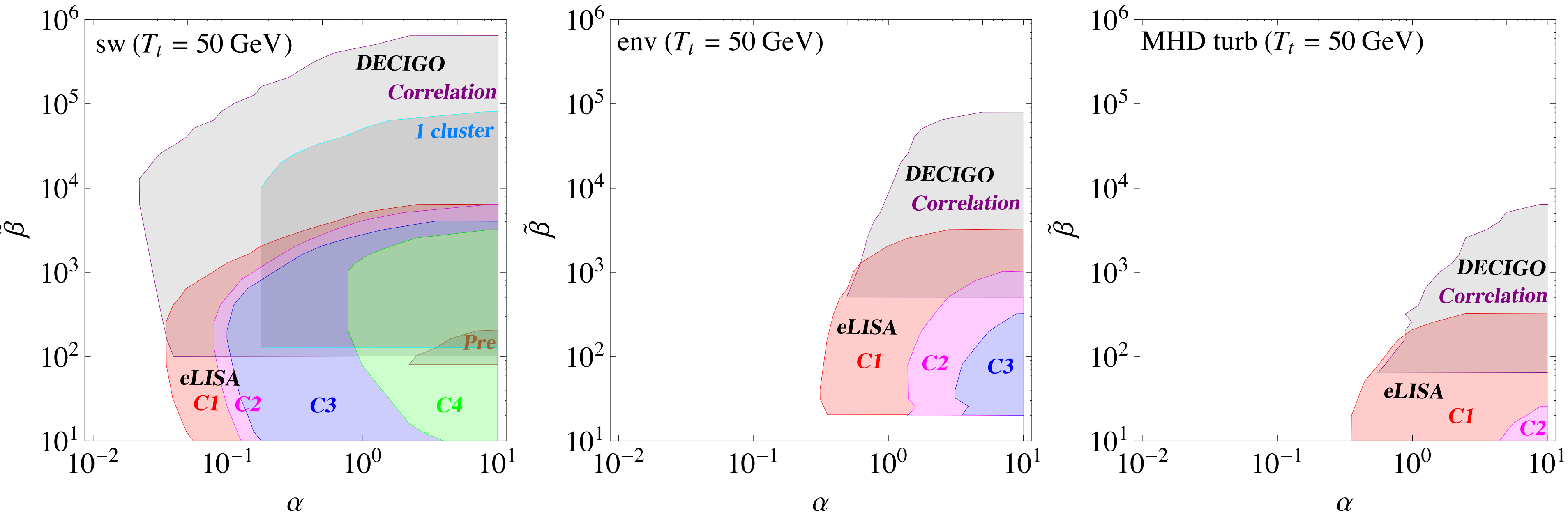

(α, βtilde)_exp. by New spectra (T_t=100GeV)

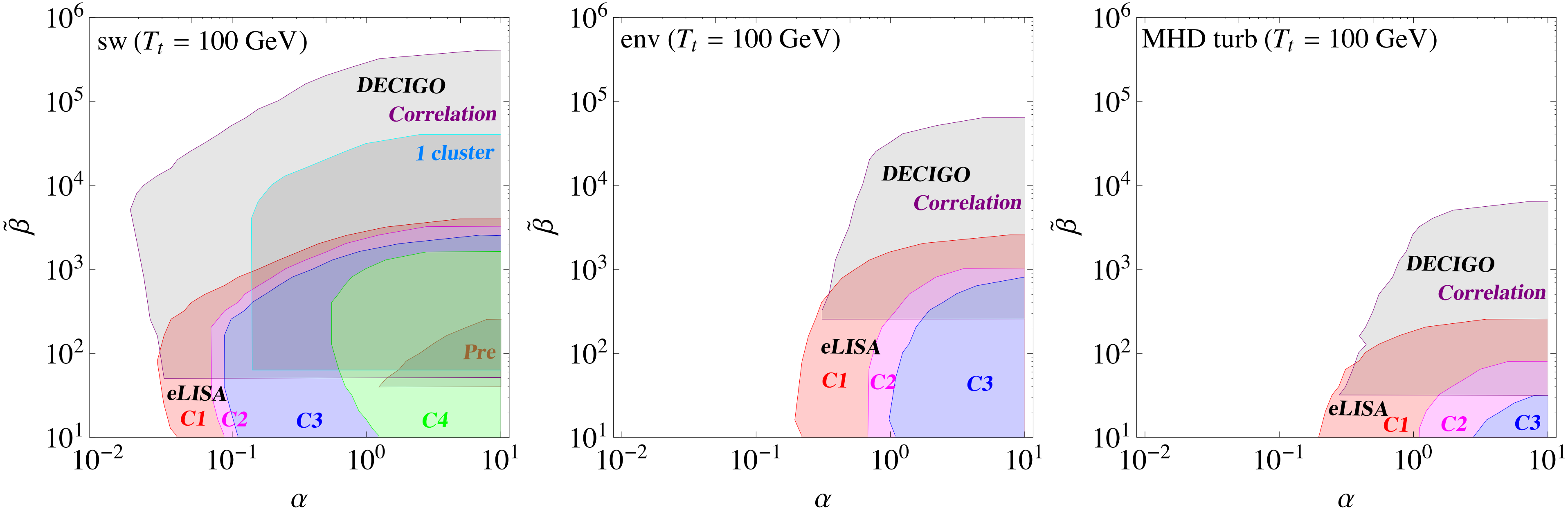

Efficiency factor κ(v_b , α)

J. R. Espinosa, *et al*, JCAP **1006**, 028 (2010)

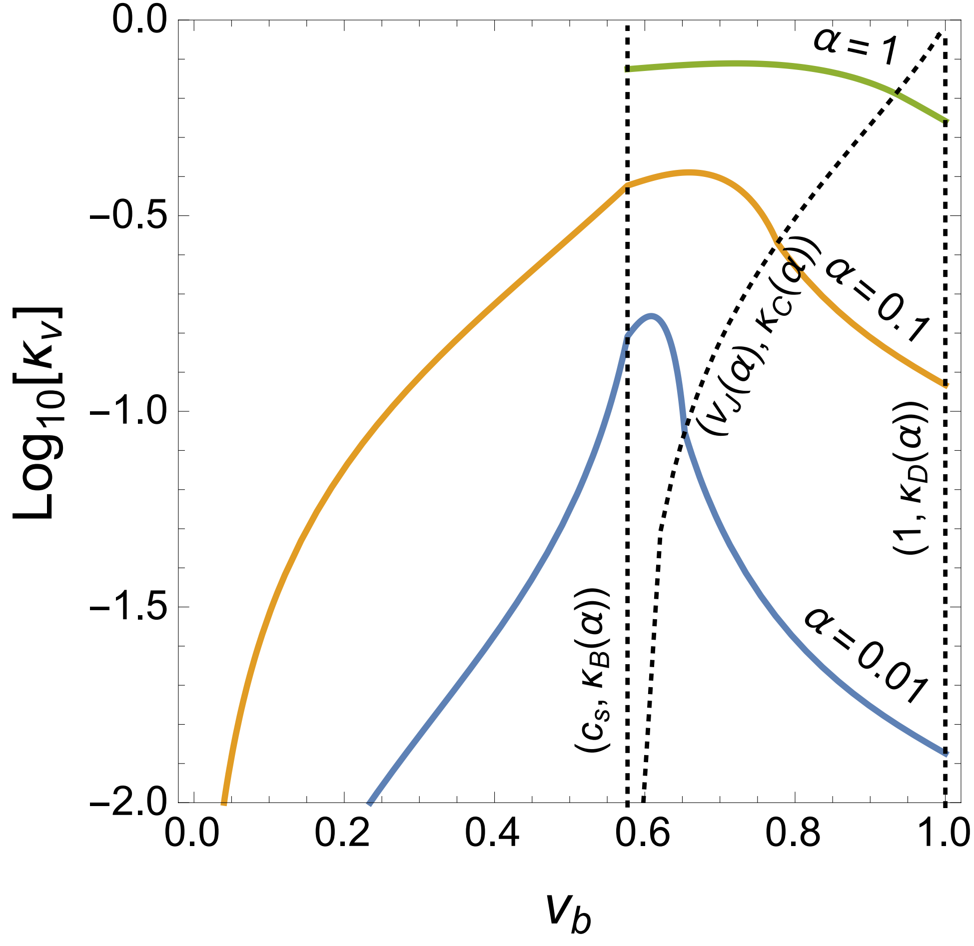

A Numerical fits to the efficiency coefficients J. R. Espinosa, *et al.*

In this section we provide fits to the numerical results of section 4. These fits facilitate the functions $\kappa(\xi_w, \alpha_N)$ and $\alpha_+(\xi_w, \alpha_N)$ without solving the flow equations and with a precision better that 15% in the region $10^{-3} < \alpha_N < 10$.

In order to fit the function $\kappa(\xi_w, \alpha_N)$, we split the parameter space into three regions and provide approximations for the four boundary cases and three families of functions that interpolate in-between: For small wall velocities one obtains ($\xi_w \ll c_s$)

$$\kappa_A \simeq \xi_w^{6/5} \frac{6.9\alpha_N}{1.36 - 0.037\sqrt{\alpha_N} + \alpha_N} . \tag{A.1}$$

For the transition from subsonic to supersonic deflagrations ($\xi_w = c_s$)

$$\kappa_B \simeq \frac{\alpha_N^{2/5}}{0.017 + (0.997 + \alpha_N)^{2/5}} . \tag{A.2}$$

ξ_J is same as our $v_b(\alpha)$

For Jouguet detonations ($\xi_w = \xi_J$), as stated in eq. (4.2)

$$\kappa_C \simeq \frac{\sqrt{\alpha_N}}{0.135 + \sqrt{0.98 + \alpha_N}} \quad \text{and} \quad \xi_J = \frac{\sqrt{\frac{2}{3}\alpha_N + \alpha_N^2} + \sqrt{1/3}}{1 + \alpha_N} . \tag{A.3}$$

And finally for very large wall velocity, ($\xi_w \to 1$) as stated in eq. (4.4)

$$\kappa_D \simeq \frac{\alpha_N}{0.73 + 0.083\sqrt{\alpha_N} + \alpha_N} . \tag{A.4}$$

For subsonic deflagrations a good fit to the numerical results is provided by

$$\boxed{\kappa(\xi_w \lesssim c_s) \simeq \frac{c_s^{11/5}\kappa_A\kappa_B}{(c_s^{11/5} - \xi_w^{11/5})\kappa_B + \xi_w c_s^{6/5}\kappa_A} ,} \tag{A.5}$$

and for detonations by

$$\boxed{\kappa(\xi_w \gtrsim \xi_J) \simeq \frac{(\xi_J - 1)^3 \xi_J^{5/2} \xi_w^{-5/2} \kappa_C \kappa_D}{[(\xi_J - 1)^3 - (\xi_w - 1)^3]\xi_J^{5/2}\kappa_C + (\xi_w - 1)^3\kappa_D} .} \tag{A.6}$$

The numerical result for the hybrid (supersonic deflagration) region is well described by a cubic polynomial. As boundary conditions, one best uses the two values of κ and the first derivative of κ at $\xi_w = c_s$. Notice that the derivative of κ in ξ_w is not continuous at the point ξ_J. The derivative at $\xi_w = c_s$ is approximately given by

$$\delta\kappa \simeq -0.9 \log \frac{\sqrt{\alpha_N}}{1 + \sqrt{\alpha_N}} . \tag{A.7}$$

This differs from the derivative one would obtain from the fit in the region $\xi_w < c_s$, but mostly for values $\alpha \gtrsim 1$, where no solutions exist for $\xi_w < c_s$. The expression for supersonic deflagrations then reads

$$\boxed{\kappa(c_s < \xi_w < \xi_J) \simeq \kappa_B + (\xi_w - c_s)\delta\kappa + \frac{(\xi_w - c_s)^3}{(\xi_J - c_s)^3}[\kappa_C - \kappa_B - (\xi_J - c_s)\delta\kappa] .} \tag{A.8}$$

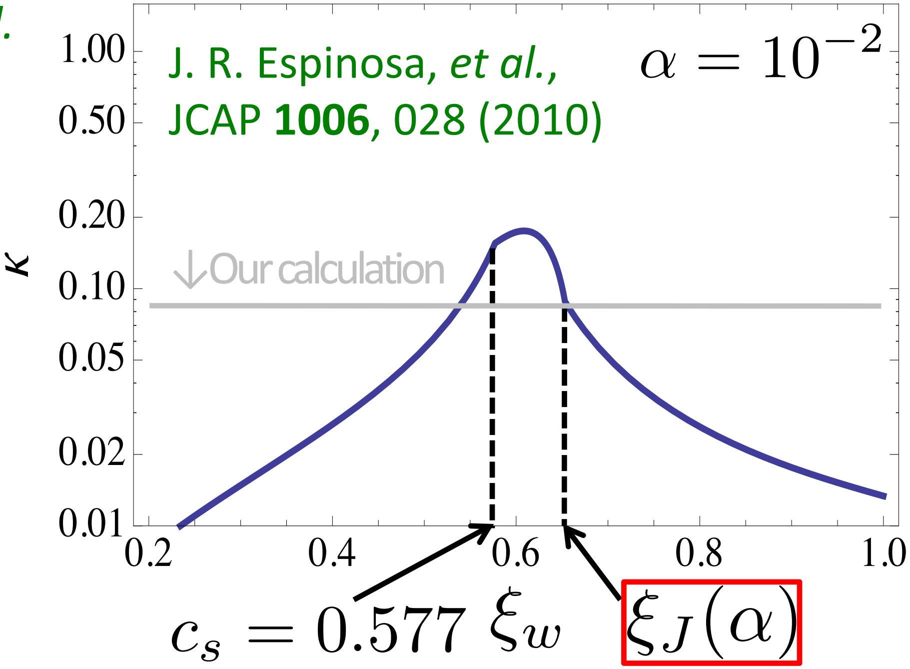

$$\tilde{\Omega}_{\rm coll} h^2 \simeq \frac{1.8 \times 10^{-6} (\kappa(\alpha, \xi_w))^2 \xi_w^3}{0.42 + \xi_w^2} \times \left(\frac{\alpha}{1+\alpha}\right)^2 \tilde{\beta}^{-2}$$

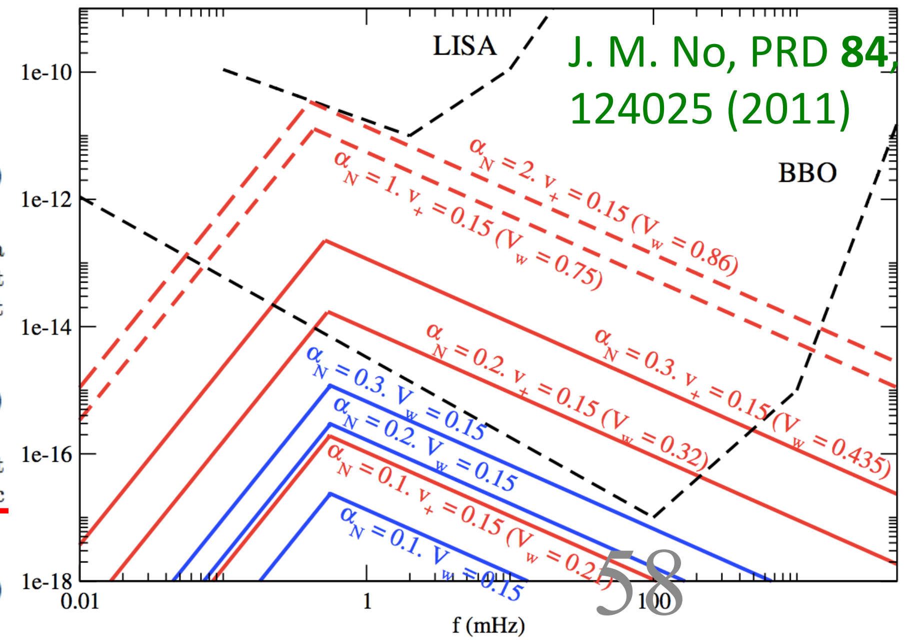

Contour plot of α on (ξ_w, v_+) plane

α is given by effective potential.

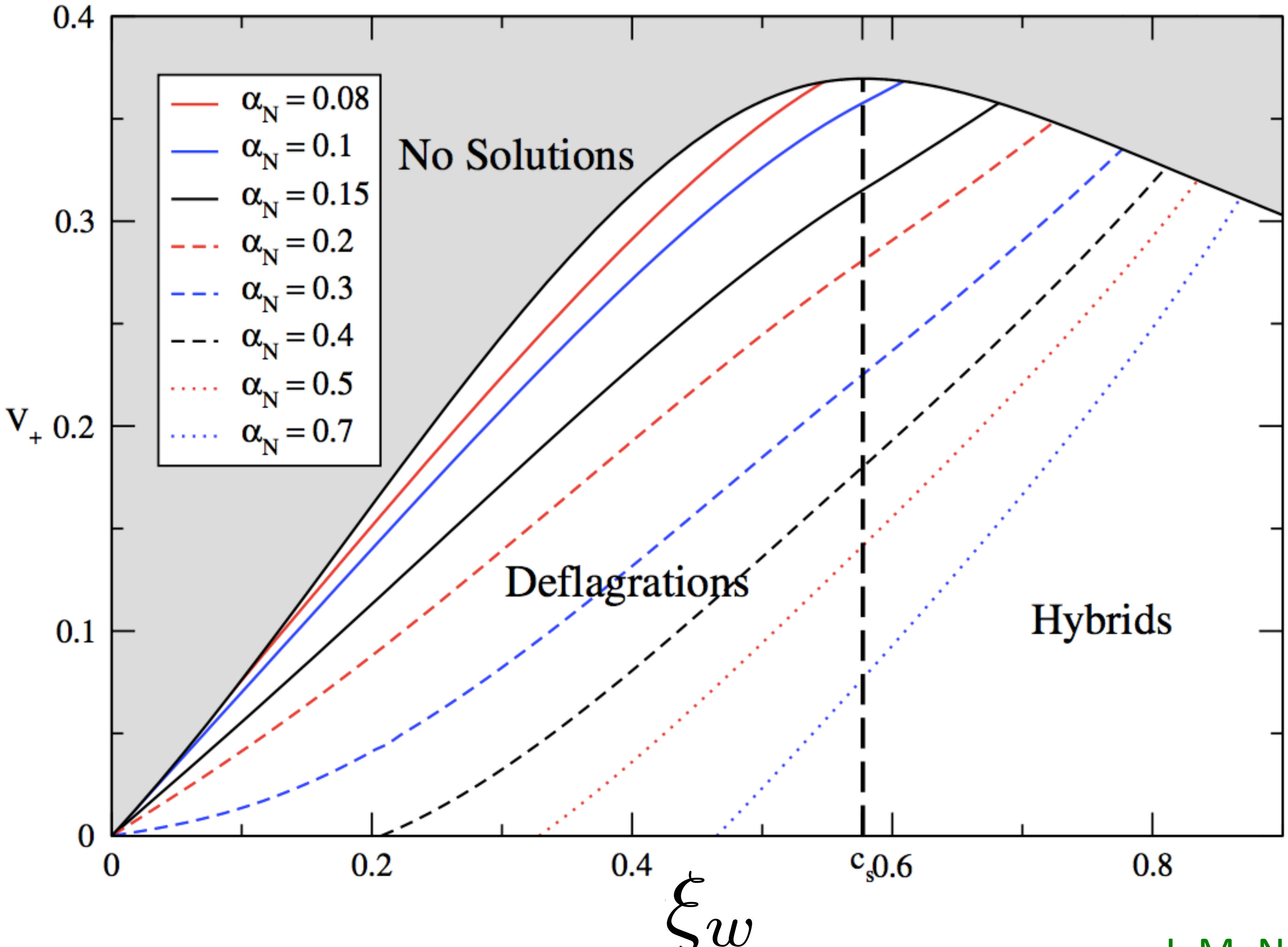

Diffusion upper bound of EWBG

EWBG requires small ξ_w
⇆GW requires large

J. M. No, PRD84, 124025 (2011)

Contour plot of v_+ on (ξ_w, α) plane

α is given by effective potential.

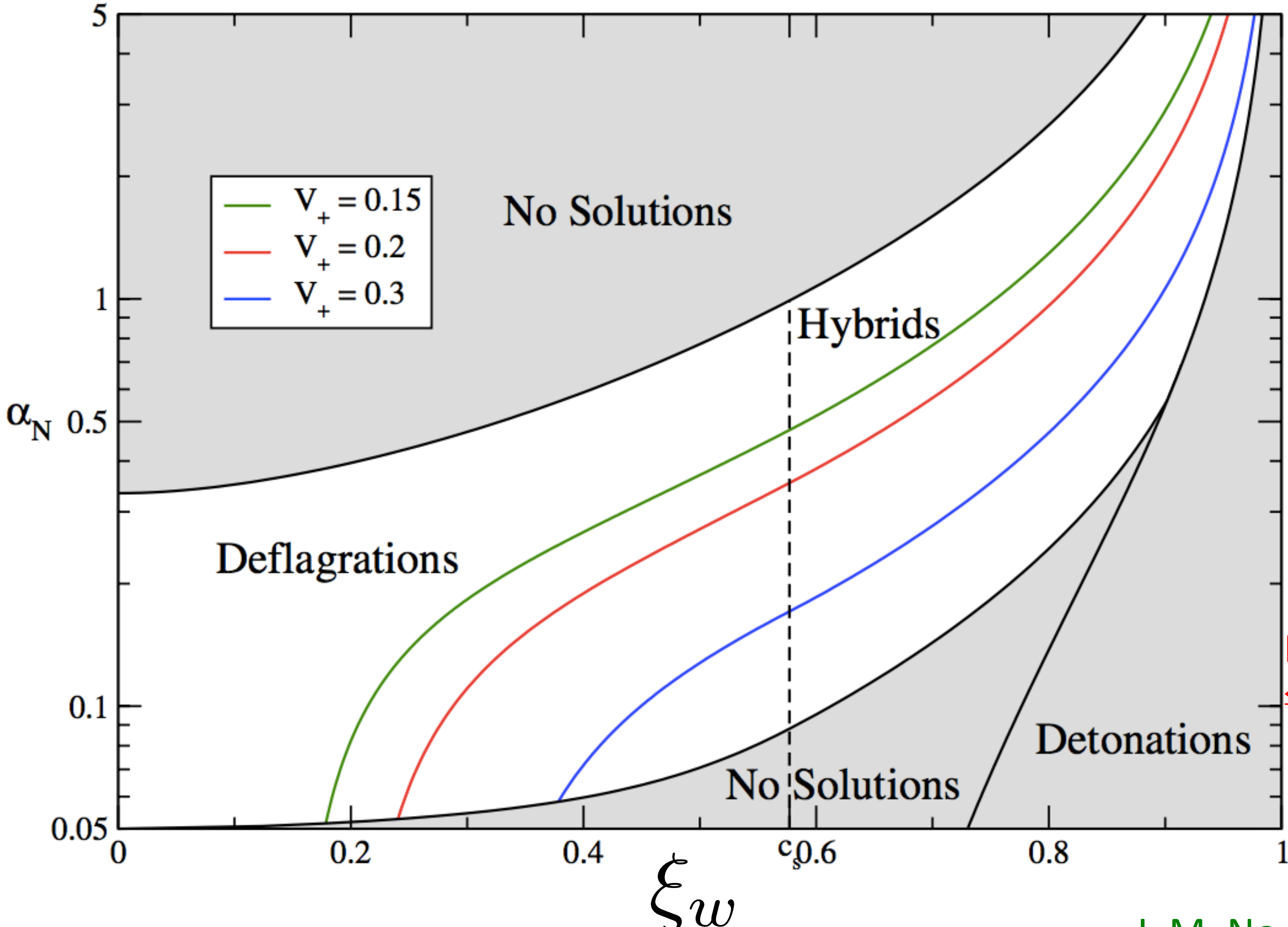

EWBG requires small ξ_w
⇆GW requires large

J. M. No, PRD84, 124025 (2011)

Foreground noise from white dwarf binaries

R. Schneider, S. Marassi, V. Ferrari, Class. Quant. Grav. **27**, 194007 (2010)

Stochastic backgrounds of gravitational waves from extragalactic sources

R Schneider[1], S Marassi[2], V Ferrari[2]

[1] INAF, Osservatorio Astrofisico di Arcetri, Largo Enrico Fermi 5, 50125, Firenze, Italy

[2] Dipartimento di Fisica G.Marconi, Sapienza Universit'a di Roma and Sezione INFN ROMA1, piazzale Aldo Moro 2, I-00185 Roma, Italy

E-mail: `raffa@arcetri.astro.it`

Abstract.

Astrophysical sources emit gravitational waves in a large variety of processes occurred since the beginning of star and galaxy formation. These waves permeate our high redshift Universe, and form a background which is the result of the superposition of different components, each associated to a specific astrophysical process. Each component has different spectral properties and features that it is important to investigate in view of a possible, future detection. In this contribution, we will review recent theoretical predictions for backgrounds produced by extragalactic sources and discuss their detectability with current and future gravitational wave observatories.